Department of Surgery

31st Annual

RESIDENT RESEARCH SYMPOSIUM

University of California San Francisco

Wednesday
April 25, 2018

Carla M. Pugh, MD, PhD

J. Englebert Dunphy Visiting Professor
Professor of Surgery & Director, Technology Enabled Clinical Improvement (T.E.C.I.) Center
Stanford University

UCSF Mission Bay
William & Susan Oberndorf Auditorium
1855 4th Street, Room A1602B
San Francisco, California

UCSF Department of Surgery Education Office Telephone:
(415) 476-1239 **Email:** EducationOffice@ucsf.edu. For more information scan code or visit: www.surgery.ucsf.edu

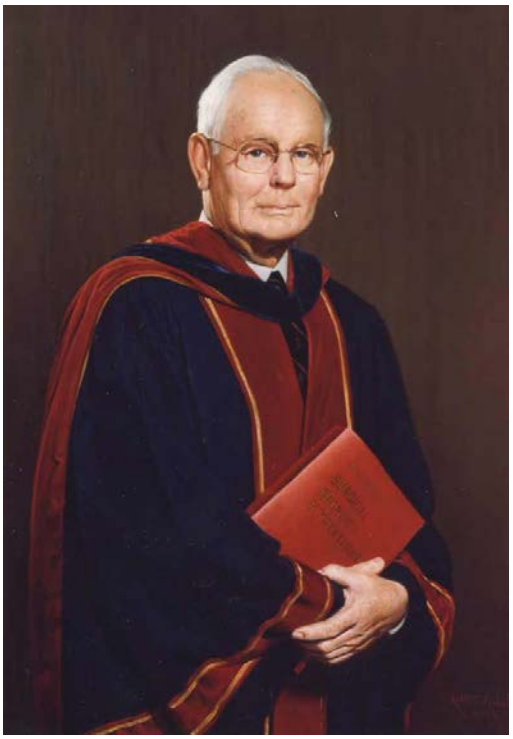

J. Englebert Dunphy, MD

Professor of Surgery and Chair of the Department from 1964 to 1975

Dr. Dunphy earned his medical degree at Harvard Medical School and completed his surgical residency training at the Peter Bent Brigham Hospital in Boston. He then joined the faculty at Harvard before accepting the position of the Chair for the Department of Surgery at the University of Oregon. In 1964, Dr. Dunphy was offered and accepted the position of the Chair for the Department of Surgery at the University of California, San Francisco. Dr. Dunphy was president of the Society of University Surgeons, the American Surgical Association, and the American College of Surgeons. He received honorary fellowships in six foreign colleges of surgeons as recognition of his international stature.

Dr. Dunphy was renowned for excellence in many aspects of surgery, with a special interest in the gastrointestinal tract. He was one of the leading surgical educators of his day, and was greatly admired and respected by his colleagues and residents. Dr. Dunphy conducted research in wound healing at a basic level. Dr. Dunphy strongly believed that prospective academic surgeons should become grounded in basic science, and he was one of the first surgical leaders in the United States to obtain an NIH training grant supporting residents in the laboratory.

2017 Dunphy Professor

Carla M. Pugh, MD, PhD

Professor, Department of Surgery, Stanford University

Carla M. Pugh, MD, PhD, FACS is Professor of Surgery at Stanford University School of Medicine. She is also the Director of the Technology Enabled Clinical Improvement (T.E.C.I.) Center. Her clinical area of expertise is Acute Care Surgery. Dr. Pugh obtained her undergraduate degree at U.C. Berkeley in Neurobiology and her medical degree at Howard University School of Medicine. Upon completion of her surgical training at Howard University Hospital, she went to Stanford University and obtained a PhD in Education. She is the first surgeon in the United States to obtain a PhD in Education. Her goal is to use technology to change the face of medical and surgical education.

Her research involves the use of simulation and advanced engineering technologies to develop new approaches for assessing and defining competency in clinical procedural skills. Dr. Pugh holds two patents on the use of sensor and data acquisition technology to measure and characterize hands-on clinical skills. Currently, over two hundred medical and nursing schools are using one of her sensor enabled training tools for their students and trainees. Her work has received numerous awards from medical and engineering organizations. In 2011 Dr. Pugh received the Presidential Early Career Award for Scientists and Engineers from President Barak Obama at the White House. She is considered to be a lead, international expert on the use of sensors and motion tracking technology for performance measurement. In 2014 she was invited to give a TEDMED talk on the potential uses of technology to transform how we measure clinical skills in medicine.

Past Visiting Professors

Bernard Langer, M.D.
Professor and Chairman of Surgery, University of Toronto
February 5-6, 1988

William Silen, M.D.
Professor of Surgery, Harvard Medical School
February 3-4, 1989

James Thompson, M.D.
Professor and Chairman of Surgery, University of Texas, Galveston
February 2-3, 1990

Murray Brennan, M.D.
Professor and Chair of Surgery, Memorial Sloan-Kettering Cancer Center
February 3-4, 1991

Richard Simmons, M.D.
Professor and Chairman of Surgery, University of Pittsburgh
January 31-February 1, 1992

Stephen F. Lowry, M.D.
Professor of Surgery, Cornell University Medical College
February 4-5, 1993

Jared Diamond, Ph.D.
Professor of Physiology, UCLA School of Medicine
February 4, 1994

Samuel A. Wells, Jr., M.D.
Professor and Chairman of Surgery, Washington University
February 17, 1995

Jonathon E. Rhoads, M.D.
Chief of Surgical Oncology, University of Pennsylvania, Philadelphia
February 16, 1996

Patricia K. Donahoe, M.D.
Chief, Pediatric Surgical Services, Massachusetts General Hospital
February 27, 1997

David L. Dunn, M.D., Ph.D.
Professor and Chairman of Surgery, University of Minnesota
February 27, 1998

Ori D. Rotstein, M.D.
Professor of Surgery, Toronto Hospital
February 26, 1999

Olga Jonasson, M.D.
Director of Education and Surgical Services Department
American College of Surgeons
March 17, 2000

Glenn Steele, Jr., M.D. Ph.D.
Dean, School of Medicine, University of Chicago
March 9, 2001

Alexander W. Clowes, M.D.
Professor of Surgery and Chairman, University of Michigan
March 7, 2002

Michael Mulholland, M.D., Ph.D.
Professor of Surgery and Chairman, University of Michigan
March 7, 2003

Christian Larsen, M.D., Ph.D.
Professor of Surgery, Emory University
March 19, 2004

Danny O. Jacobs, M.D., M.P.H.
Chair, Department of Surgery, Duke University Medical Center
March 4, 2005

Steven D. Leach, M.D.
Chief of Surgical Oncology, Johns Hopkins University
March 3, 2006

M. Judah Folkman, M.D.
Professor of Pediatric Surgery & Cell Biology, Harvard Medical School
Director, Vascular Biology Program, Children's Hospital, Boston
February 15-16, 2007

Sir Peter Morris, AC, FRS, FRCS
Director, Centre for Evidence in Transplantation
Royal College of Surgeons of England
April 4, 2008

George K. Gittes, M.D.
Chair of Pediatric Surgery, University of Pittsburgh
April 3, 2009

Joseph P. Vacanti, M.D.
Chief, Pediatric Surgery, Massachusetts General Hospital
March 12, 2010

Maria Bertagnolli, M.D.
Professor of Surgery, Harvard
Chief, Surgical Oncology, Brigham and Women's Hospital
April 1, 2011

Michael Harrison, M.D.
Director Emeritus, Fetal Treatment Center, Professor of Pediatric Surgery,
University of California, San Francisco
April 13, 2012

Martin Elliott, M.D.
Professor of Cardiothoracic Surgery, University College London
April 5, 2013

Clifford Ko, M.D.
Director, Division of Research and Optimal Patient Care
Director, National Surgical Quality Improvement Program (ACS NSQIP)
American College of Surgeons
April 25, 2014

Jennifer Grandis, M.D.
Associate Vice Chancellor, Clinical and Translational Research
Director, Clinical and Translational Science Institute (CTSI)
Professor of Otolaryngology, University of California San Francisco
March 11, 2015

Robert C. Robbins, M.D.
President and Chief Executive Officer
Texas Medical Center
April 27, 2016

Samuel RG Finlayson, M.D., MPH
President and Chair, Department of Surgery
University of Utah
April 12, 2017

2017 Symposium Winners

From left to right: John Roberts, Catherine Juillard*, Steven Wisel, Yvonne Kelly, Samuel Finlayson, Kathryn Chomsky-Higgins, Jeremy Sharib and Peter Stock

BEST ABSTRACT PRESENTATION – Kathryn Chomsky-Higgins, MD, MS
Less Is More: Cost-Effectiveness Analysis of Surveillance Strategies for Small, Nonfunctional, Radiographically Benign Adrenal Incidentalomas

OUTSTANDING ABSTRACT PRESENTATION – S. Ariane Christie, MD
Injury and Care-Seeking in Southwest Cameroon: A Community Based Survey
**Catherine Juillard accepted award on behalf of S. Ariane Christie.*

OUTSTANDING ABSTRACT PRESENTATION – Steven Wisel, MD
Optimization of a Polycaprolactone (PCL) Scaffold for Islet and Cellular Transplantation

BEST QUICK-SHOT PRESENTATION – Yvonne Kelly, MD
An Evidenced-Based Approach to the Identification and Treatment of Severe Acute Cholecystitis -Beyond the Tokyo Guidelines

OUTSTANDING QUICK-SHOT PRESENTATION – Jeremy Sharib, MD
Minimally Invasive Classification of Pancreatic Cystic Neoplasms

9:00 AM **Welcome Remarks**
Julie Ann Sosa, MD, MA, FACS, Leon Goldman, MD Distinguished Professor & Chair, UCSF Department of Surgery

Introduction
Peter Stock, MD, PhD, Professor of Surgery & Chair, Research Committee, UCSF Department of Surgery

SESSION 1: TRANSPLANT, IMMUNOLOGY & STEM CELLS

Moderator: Garrett Roll, MD , Assistant Professor of Surgery

9:05 AM **Definitive Characterization of Extrathymic AIRE-expressing cells (eTACS)**
Jhoanne Bautista, MD, PhD, 1st Year Research Fellow

9:15 AM **Comparative Analysis of Alloantigen-Stimulated Gene Expression in HIV+ Transplant Rejectors versus Non-Rejectors**
Simon Chu, MS, Medical Student

9:25 AM **Defining Hepatocyte Plasticity in a Faithful Animal Model of Human Acute Liver Injury**
Hubert Luu, MD, MS, 2nd Year Research Fellow

9:35 AM **CRISPR Knockout Screens in Primary Human Lymphocytes to Determine Foxp3 Stability**
Oren Shaked, MD, 1st Year Research Fellow

9:45 AM **Preservation of Pancreatic Islet Grafts and Reversal of Diabetes Using Novel Parathyroid Cotransplantation**
Casey Ward, MD, 1st Year Research Fellow

9:55 AM **Hematopoietic Stem Cell Transplantation Using a Non-Toxic Regimen to Ablate the Fetal Bone Marrow Niche Enables Engraftment of Brain Microglial Cells**
Quoc-Hung Ly Nguyen, MD, 1st Year Research Fellow

10:05 AM **Living Donor Liver Transplantation for Alcoholic Liver Disease: The North American Experience**
Hillary Braun, MD, Resident, PGY2

10:10 AM **Developing a Murine Model to Study Novel Therapies for Tolerance in Vascular Composite Tissue Allotransplantation**
Nicole Conkling, MD, 2nd Year Research Fellow

10:15 AM ***Break***

SESSION 2: VASCULAR, TRAUMA, SEPSIS & CANCER

Moderator: Johannes Kratz, MD, Assistant Professor of Surgery

10:30 AM **Active Surveillance Versus Immediate Resection For Non-Functioning Pancreatic Neuroendocrine Tumors: A Cost-Effectiveness Analysis**
Kathryn Chomsky-Higgins, MD, MS, 2nd Year Research Fellow

10:40 AM **Tumor Infiltrating Lymphocyte Directed Neoadjuvant Therapy in Operable Stage III Melanoma**
Kelly Mahuron, MD, 2nd Year Research Fellow

10:50 AM **An Improved Method of Minimally Invasive Pulmonary Metastasectomy that Allows Full Palpation of the Lung Without Chest Wall Disruption**
Greg Haro, MD, 1st Year Research Fellow

11:00 AM **Mechanisms of Facial Fracture in the Homeless at an Urban Level I Trauma Center**
Audrey Nguyen , MD, 1st Year Research Fellow

11:10 AM **The Impact of Pro-Inflammatory States on the Fibrin-Platelet Balance Following Injury**
Anamaria Robles, MD, 2nd Year Research Fellow

11:20 AM **Cost Burden of Overtreating Low Grade Pancreatic Cystic Neoplasms**
Jeremy Sharib, MD, 2nd Year Research Fellow

11:30 AM **Tissue Factor Targeted Nanoparticles for the Prevention of Neointimal Hyperplasia Following Vascular Intervention**
Evan Werlin, MD, 2nd Year Research Fellow

11:40 AM **The Ex Vivo Perfused Human Lung as a Model of Acute Lung Injury in Sepsis**
James Ross, MD, 1st year Research Fellow

11:45 AM **Hyponatremia and Complex Biliary Disease**
Michael Zobel, MD, Resident, PGY3

11:50 AM ***Lunch Break Gourmet boxed lunches provided***

SESSION 3: TECHNICAL INNOVATION, GLOBAL SURGERY/PUBLIC HEALTH & EDUCATION

Moderator: Amar Nijagal, MD, Assistant Professor of Surgery

1:10 PM **Optimization and Validation of the Economic Clusters Model for Facilitating Health Disparities Research in Low-Resource Settings**
Lauren Eyler, MD, MPH, Resident, PGY2

1:20 PM **Residents Learning Robotic Technology: Turning a Complicated Process Into an Opportunity for Progress**
Courtney Green, MD, 2nd Year Research Fellow

1:30 PM **Preclinical Surgical Experience with an Intervascular Hemofilter for Organ Replacement Therapy**
Jarrett Moyer, MD, 2nd Year Research Fellow

1:40 PM **Machine Learning Without Borders? An Adaptable Tool to Optimize Mortality Prediction in Diverse Clinical Settings**
S. Ariane Christie, MD, 3rd Year Research Fellow

1:50 PM **A Magnetic Jejunoileal Partial Diversion in Nonhuman Primates: A Novel Approach in Metabolic Surgery**
Veeshal Patel, MD, MBA, 1st Year Research Fellow

1:55 PM **The Impact of Incisional Negative Pressure Wound Therapy on Wound Healing Complications in the Groin**
Clara Gomez-Sanchez, MD, 1st Year Research Fellow

2:00 PM ***Break***

2:15 PM **Keynote: Hacking Healthcare with Sensors: Unfolding the Metrics of Physician Expertise**
Carla M. Pugh, MD, PhD, Dunphy Visiting Professor

3:15 PM **Closing Remarks & Awards Presentation**
Peter Stock, MD, PhD, Research Committee Chair

Definitive Characterization of Extrathymic AIRE-expressing cells (eTACs)

Jhoanne Bautista MD PhD, Jay Gardner MD PhD, Jennifer Liu PhD, Benjamin Yuen PhD, Mark S. Anderson MD PhD

INTRODUCTION:

Extrathymic AIRE-expressing cells (eTACs) are bone marrow-derived cells that express the Autoimmune Regulator protein and are found in secondary lymphoid organs in both mice and humans. They appear to enforce tolerance to self antigens in the periphery by deleting autoreactive CD8+ (killer) T cells and by rendering autoreactive CD4+ (helper) T cells anergic or unresponsive to T cell receptor (TCR) stimulation, thereby preventing autoimmune attacks on pancreatic beta islets that leads to diabetes. These cells have great potential as therapy for autoimmune disease and may potentially mediate allograft tolerance in solid organ transplantation. However, these cells must first be definitively characterized and their differentiation lineage determined in order to expand, isolate, and prepare them for adoptive transfer therapy.

METHODS:

Briefly, we used a combination of single cell sorting, flow cytometry and transcriptome analysis of mRNA libraries we generated using single cell RNA sequencing to identify and characterize eTACs in a mouse model where AIRE expression is marked with co-expression of the fluorescent protein, GFP. Machine learning algorithms were then used to identify cell clusters based on their differential gene expression patterns, and also to generate models that trace eTAC lineage from bone-marrow derived precursors.

RESULTS:

We found that two distinct cell populations may express the AIRE protein in the periphery: a distinct subset of migratory dendritic cells and a few random B cells. We believe that the specialized dendritic cells represent the tolerogenic eTAC population because these are the cells previously found in the lymph node paracortical region that where AIRE expression is validated at the protein level using immunofluorescence.

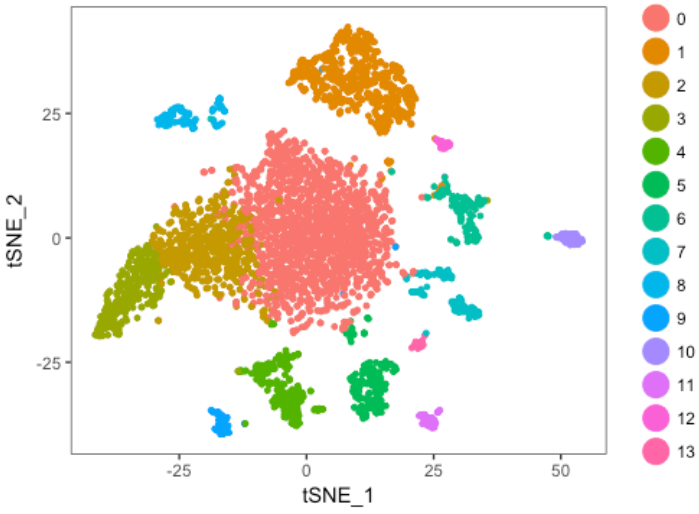

CONCLUSIONS:

Work is underway to validate the models we generated using machine learning with reporter mice that trace the lineage of AIRE-expressing cells. We are also working on definitively identifying the robust, and arguably redundant signaling mechanisms that eTACs used to enforce tolerance.

Comparative Analysis of Alloantigen-Stimulated Gene Expression in HIV(+) Transplant Rejectors versus Non-Rejectors

Simon N Chu[2,3], Karim Lee[1], Casey Ward[1], Peter G Stock[1], Qizhi Tang[1]

[1]Department of Surgery, University of California, San Francisco
[2]School of Medicine, University of California, San Francisco
[3]Howard Hughes Medical Institute, University of California, San Francisco

Purpose: In a multi-center prospective trial of solid-organ transplantation in persons with HIV, recipients had a 2-3x increased rejection rate when compared to historical data on HIV(-) recipients. Immunological correlates of rejection in this population have not previously been identified. Here, we perform alloantigen-stimulated gene expression profiling to investigate functional differences between HIV(+) rejectors and non-rejectors.

Methods: Donor and recipient specimens were collected prior to transplant. Rejectors (R) were selected based on biopsy-proven acute cellular rejection within 3 months of transplant. Non-rejectors (NR) were selected based on lack of clinical and biopsy-proven rejection. Propensity scores were matched between R and NR to reduce bias from confounding variables. Third party was selected from a healthy donor with a high number of HLA mismatches. CD40L-stimulated donor or third party B cells were used to stimulate recipient cells *in vitro* prior to gene expression analysis of 800 genes using a custom NanoString panel. Raw counts were normalized and p-values were adjusted using the Benjamini-Hochberg procedure for multiple testing correction.

Results: Rejectors (n=2) showed high expression of T cell co-stimulators CD28 and ICOS (FC=2.31, 2.10; p=0.0242, 0.0334), well-known targets of checkpoint blockade in transplantation. Interestingly, NR (n=2) exhibited high differential expression of genes associated with the complement system, including C1QA, C1QB, C2, CFB, and SERPING1 (FC=13.55, 10.70, 3.03, 2.85, 3.56; p=0.0027, 0.0099, 0.0444, 0.0429, 0.016). Moreover, the leukocyte immunoglobulin-like receptor (LILR) family of receptors LILRB4, LILRB1, and LILRA1 were also upregulated (FC=3.32, 3.20, 3.27; p=0.0384, 0.017, 0.0317) in NR vs R. Differential gene expression between rejectors and non-rejectors was preserved irrespective of stimulus by either donor or 3rd party.

Conclusions: Overall, our results suggest that increased rates of rejection in HIV(+) transplant recipients correlate with pre-transplant, recipient-specific immune dysfunction. Concordance in gene expression profile following stimulation with donor or 3rd party suggests that differential gene expression is an intrinsic, recipient-driven propensity to immune activation in rejectors and immune regulation in non-rejectors. HIV(+) recipients with no rejection had higher expression of complement and LILR genes. These pathways have been implicated in facilitating immune cell tolerance. C1q is reported to play a fundamental role in facilitating apoptotic cell clearance and mediating immune suppression. LILRs have been shown to suppress T-cell activation via the induction of tolerogenic DCs. Expanded analysis using this approach is warranted.

Defining Hepatocyte Plasticity in a Faithful Animal Model of Human Acute Liver Injury

Hubert Luu, M.D. M.S.; Carlos Corvera, M.D.; Holger Willenbring, M.D. Ph.D.

Acquired biliary injury from toxin ingestion, infection, or autoimmune diseases can cause liver fibrosis and failure. In this setting, liver transplantation is the gold standard of cure, but is limited by organ shortage, surgical morbidity and mortality, and complications of immune suppression. Work from our lab shows that hepatocytes can transdifferentiate into functional biliary epithelial cells (BECs) and form bile ducts, as evidenced by genetic hepatocyte fate tracing in a mouse model of Alagille syndrome, which is caused by genetic deficiency of NOTCH signaling and typically manifests soon after birth. To answer the question of whether hepatocyte transdifferentiation occurs in acquired biliary diseases in the adult, we used a rat model of extensive bile duct loss harnessing the biliary-specific toxicity of diaminodiphenyl methane (DAPM). To determine whether hepatocytes contribute to bile duct regeneration in these animals, we established genetic hepatocyte fate tracing in rats.

Methods:

Optimizing diaminodiphenyl methane (DAPM) toxicity:

To confirm and establish optimal dosing for BEC toxicity, Long-Evans hooded (LEH) wildtype rats (males, 200 grams) were given three intraperitoneal (IP) injections of DAPM ranging between 50-150 mg/kg. Serum was collected before any injection, 24 hours after the final injection, and again at 5 days. Livers were collected at 5 days for analysis of bile duct injury and loss with H&E staining and immunofluorescence.

Genetic hepatocyte fate tracing in DAPM-treated rats:

R26R-tdTomato-transgenic Cre reporter rats (Horizon Discovery; male rats weighing 200 grams) were intravenously injected with 5.5×10^{12} viral genomes of a vector AAV8-TBG-Cre (UPENN Vector Core), leading to specific and constitutive activation of tdTomato expression in hepatocytes. 1 week later, rats were given 3 intraperitoneal injections of DAPM at 100 mg/kg. Livers were collected at days 30 and 60 after the final DAPM injection for analysis of bile duct injury and loss.

Results: 24 hours after the third injection of DAPM, rats were found to have a significantly elevated serum alkaline phosphatase (AP), total bilirubin (TB), and AST (aspartate aminotransferase). By day 5, AST normalized while AP and TB remained significantly elevated. H&E staining of formalin-fixed paraffin-embedded liver sections after 5 days of injury displayed periportal hepatocellular and ductal inflammation and morphologic evidence of ductal injury and luminal de-epithelialization. Cre-mediated expression of tdTomato was highly efficient and seen in over 80% of all hepatocytes and no BECs before DAPM toxicity. Immunofluorescence staining of liver sections 30 days after DAPM injury demonstrated co-expression of the biliary marker wide-spectrum cytokeratin (wsCK) with the hepatocyte-derived tdTomato, though this effect was no longer seen at 60 days after injury.

Conclusions: In the setting of acute toxic biliary injury, mature hepatocytes contribute to biliary regeneration up to 30 days after injury, though this regenerative potential appears limited beyond this period. We are performing studies to investigate BEC regeneration at higher degrees of biliary injury and at later time points post-injury.

CRISPR Knockout Screens in Primary Human Lymphocytes to Determine Foxp3 Stability

Oren Shaked, Jessica Cortez, Alexander Marson

Introduction: Foxp3 is a transcription factor that is both necessary and sufficient in establishing regulatory T cell (Tregs) suppressive activity. Modulation of the Foxp3 master regulator has broad implications for the management of many conditions, including post-transplant immunosuppression, as well as cancer therapies. Recent evidence in a murine model has demonstrated that Foxp3 stability is in part dictated by ubiquitylation/deubiquitilation enzymes, but it is unclear what role such post-translational modifications play in the stability of Foxp3 in human Tregs. In the upcoming era of precision medicine, precision understanding of biologic functions is necessary for the design and implementation of targeted therapies.

Methods: A list of ubiquitylating and deubiquitylating enzymes was curated using GO annotations from the Gene Ontology Consortium. These were cross-referenced with sites of active mRNA transcription in Tregs from the BLUEPRINT project. Using Clustered Regularly Interspaced Short Palindromic Repeats (CRIPSR) guides, highly specific and reproducible knockouts were introduced in human Tregs from healthy human donors, after expanding these cells in tissue culture according to previously established Good Manufacturing Practices. Expressions of phenotypic markers associated with Treg functionality were assessed using flow cytometey, including Foxp3, CTLA-4, IFNγ, Helios, IL-2, IL-4, IL-10, and IL-17a.

Results: Over 1000 target genes were identified as having ubiquitylating or deubiquitylating functions in human cells, with most expressed to some degree in human Tregs. Preliminary knockouts were performed on Stub1 and USP7 to establish a workflow and demonstrate the activity of these enzymes in regulating Treg stability. As hypothesized, Stub1 knockouts increased the stability of Foxp3 expression compared to control (68.3% vs 57.2%), and USP7 knockout was associated with decreased Foxp3 expression compared to control (14.6% vs 67%)

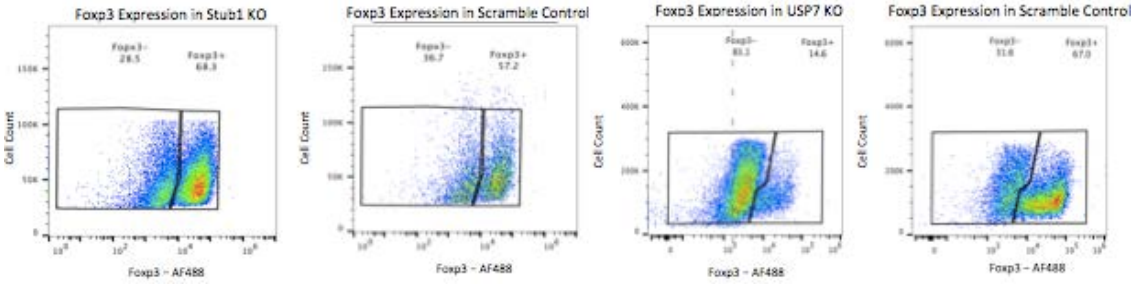

Conclusions: E3-ligases (e.g. Stub 1), and DUBs (e.g. USP7) appear to play a role in stabilizing Foxp3 expressing in human Tregs. Given the logistical challenges associated with performing an arrayed screen on approximately 1000 genes, a pooled CRISPR screen is required to identify likely targets for more specific analysis using an arrayed approach.

Preservation of Pancreatic Islet Grafts and Reversal of Diabetes using Novel Parathyroid Gland Co-Transplantation in the Extra-Hepatic Space.

Casey Ward[1], Gaetano Faleo[1], Greg Szot[1], Gopika Nair[2], Vinh Nguyen[1], Charity Juang[2], Quan-Yang Duh[3,4], Mathias Hebrok[2], Wenhan Chang[4], Peter Stock[1], Qizhi Tang[1,2]

[1] UCSF Department of Surgery, Division of Transplant Surgery
[2] UCSF Diabetes Research Center
[3] UCSF Department of Surgery, Division of Endocrine Surgery
[4] San Francisco Veteran Affairs Medical Center, Division of Endocrinology

Introduction:

Islet transplantation can cure type 1 diabetes; however, multiple donors are often needed to achieve insulin independence due to extensive perioperative loss of islets from ischemic injury. In comparison, parathyroid gland (PTG) auto and allo-transplantation in the subcutaneous (SQ) and intra-muscular (IM) sites is an established successful surgical procedure and its efficacy has been attributed to the neoangiogenic property of a unique CD34+ progenitor cell population. In this study, we aim to exploit the properties of PTG-derived CD34+ cells for the preservation of mature mouse and human islet and stem-cell-derived insulin-producing cells (SCIPC).

Materials and Methods:

Luciferase-expressing mouse islets were co-transplanted with or without PTG in the SQ and IM of syngeneic recipients. Luciferase-expressing human SCIPC grafts and human islets from deceased donors with or without cryopreserved human PTG were co-transplanted in SQ and IM of immunodeficient NSG mice. CD34+ and CD34- cells were sorted using fluorescence-activated cell sorting. Mice were made diabetic using streptozocin. Graft mass was quantified using bioluminescence imaging in recipients of luciferase expressing grafts.

Results and Discussion:

Co-transplantation of PTG with both mouse islets and human SCIPC in the SQ and IM resulted in complete preservation (>100%) of the transplanted grafts in comparison to significant islet loss in mouse islet alone (10%-SQ, 20%-IM) (Figure 1A) or SCIPC alone grafts (40%-SQ, 50%-IM) (Figure 1B) after 14 days ($p < 0.05$). Furthermore, only SCIPC+PTG co-transplanted grafts in IM achieved sustained diabetes reversal after 6 weeks. Similarly, PTG co-transplantation with a sub-optimal mass of mature human islets (1000IEQ) achieved diabetes reversal in NSG mice. After 21 days, 67% (IM) and 75% (SQ) of PTG co-transplanted mice remained diabetes free compared to 0% of mice with islets alone in SQ and IM (Figure 1C).

To elucidate the mechanism of this phenomenon further, PTG derived CD34+ progenitors and CD34- cells were co-transplanted with SCIPC grafts. The SCIPC+CD34+ co-transplant recapitulated complete preservation of graft and SCIPC function as seen with whole PTG co-transplanted grafts (Figure 2). Further, PTG derived CD34+ cells secrete proangiogenic factors and pro-islet hormones that significantly reduced islet cell death upon ex-vivo ischemia challenge.

Conclusion:

We show for the first time that co-transplantation of PTG with mature islets and stem-cell-derived beta cells leads to increased survival and diabetes reversal in the SQ and IM. Furthermore, the islet-protective activities of PTG resides in a small subpopulation of CD34+ progenitor cells. Our findings support the testing of PTG co-transplantation for improving engraftment of auto, allo, xeno, and stem-cell-derived islet transplants in future clinical trials.

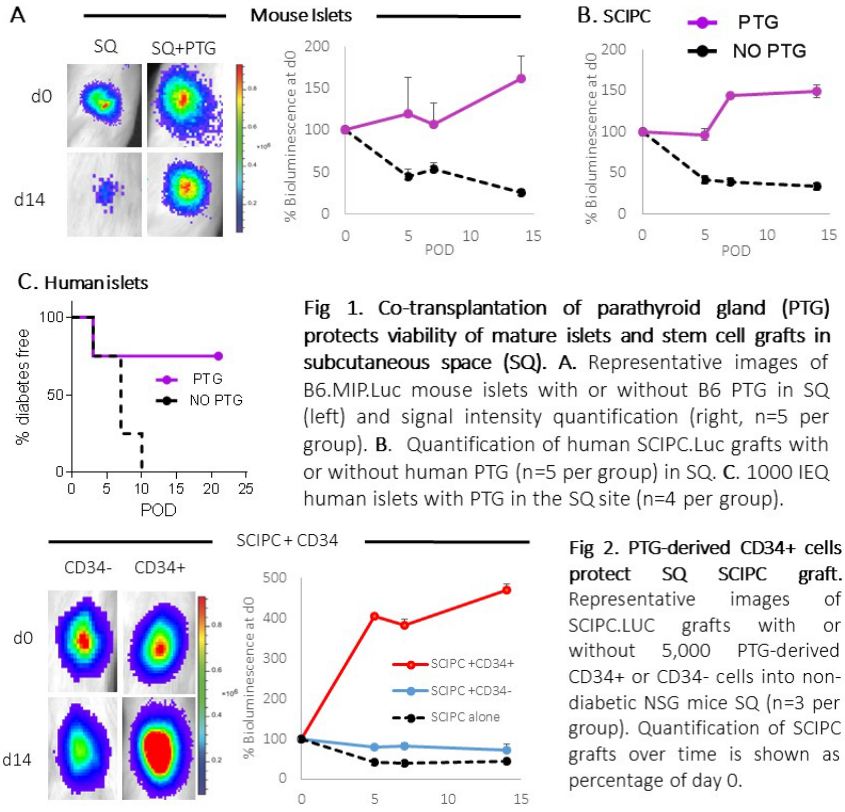

Fig 1. Co-transplantation of parathyroid gland (PTG) protects viability of mature islets and stem cell grafts in subcutaneous space (SQ). A. Representative images of B6.MIP.Luc mouse islets with or without B6 PTG in SQ (left) and signal intensity quantification (right, n=5 per group). **B.** Quantification of human SCIPC.Luc grafts with or without human PTG (n=5 per group) in SQ. **C.** 1000 IEQ human islets with PTG in the SQ site (n=4 per group).

Fig 2. PTG-derived CD34+ cells protect SQ SCIPC graft. Representative images of SCIPC.LUC grafts with or without 5,000 PTG-derived CD34+ or CD34- cells into non-diabetic NSG mice SQ (n=3 per group). Quantification of SCIPC grafts over time is shown as percentage of day 0.

Hematopoietic Stem Cell Transplantation Using a Non-Toxic Regimen to Ablate the Fetal Bone Marrow Niche Enables Engraftment of Brain Microglial Cells

Quoc-Hung L. Nguyen, MD[1,2], Russell G. Witt, MD[1,2], Bowen Wang[2], Jeremy Shea[3], Saul Villeda[3], Tippi C. MacKenzie, MD[1,2]

[1] The Center for Maternal-Fetal Precision Medicine, University of California, San Francisco, CA
[2] The Department of Surgery, University of California, San Francisco, CA
[3] The Department of Anatomy, University of California, San Francisco, CA

Introduction: Using hematopoietic stem cell (HSC) transplantation to correct diseases affecting neurological function requires microglial cell engraftment. Although phenotypic improvement has been reported in diseases such as Friedrich's ataxia, most strategies involve potentially morbid irradiation. Our group uses antibody-based regimens to condition host bone marrow without irradiation prior to transplantation, and we now assess whether this strategy enables brain microglial cell engraftment.

Methods: We depleted fetal bone marrow HSCs using an antibody against the Ckit receptor (ACK2), with and without a second antibody against CD47 (MIAP410) to improve clearance of affected HSCs (with saline-injected controls). At birth, pups were transplanted with congenic HSCs. Engraftment levels in blood were measured every 4 weeks, and mice with highest chimerism were harvested at 32 weeks to look for donor-derived $CD45^{lo}CD11b^{hi}$ microglia (after perfusion).

Results: The blood chimerism levels in animals that received in utero ablation were higher than those that did not (26.5% vs 6.6%, n=15 p=0.02). The brains of 4 chimeras (27.1 $\pm$ 12.8% chimerism in blood; 20.9 $\pm$ 7.9% chimerism in bone marrow) were analyzed and donor-derived microglia were successfully detected by flow cytometry (**Fig. 1).**

Conclusion: Our strategy of neonatal HSC transplantation using a non-toxic antibody-based approach results in clinically relevant levels of circulating chimerism, with evidence of engraftment in the brain. This strategy may be relevant for prenatally diagnosed diseases with neurological symptoms such as inborn errors of metabolism. We are currently performing immunohistochemistry to further characterize the levels of engraftment in specific regions of the brain.

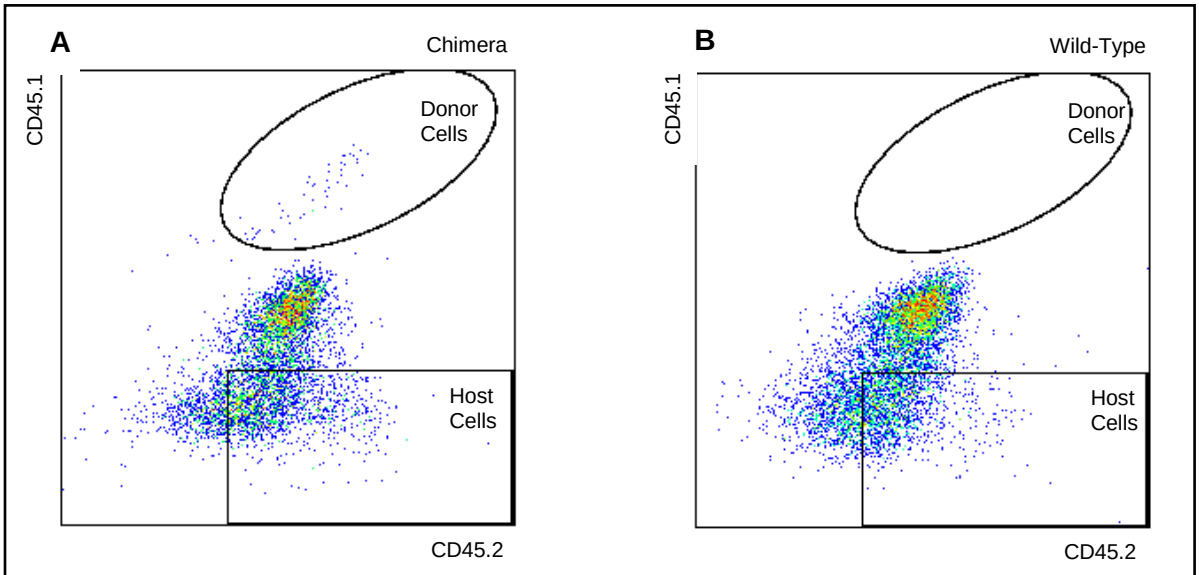

Fig 1. Flow cytometry gating strategy. Initial gating is on live, mononuclear, CD11b+ cells, followed by CD45.1 x CD45.2. Chimera is positive for donor microglia (A), while wild-type control is not (B). 0

Living Donor Liver Transplantation for Alcoholic Liver Disease: The North American Experience

Braun HJ, Dodge JL, Grab JD, Syed SM, Roll GR, Freise CE, Roberts JP, Ascher NL

Introduction: Alcoholic liver disease (ALD) is now a well-recognized indication for liver transplantation, however the literature on living donor liver transplantation (LDLT) for ALD is sparse and primarily from single Asian transplant centers. Here, we report LDLT outcomes for ALD from the Adult-to-Adult Living Donor Liver Transplantation Study (A2ALL), comprising data from nine transplant centers in North America.

Methods: Demographics and outcomes of donors and recipients in the A2ALL study who underwent LDLT between April 1998 and January 2014 were reviewed. We compared recipients with ALD and non-ALD diagnoses using Wilcoxon rank sum and chi-squared tests; graft and patient survival were estimated using Kaplan-Meier methods and compared by the log-rank test.

Results: 1065 donor/recipient pairs were included. 168 (15.8%) recipients underwent LDLT for ALD; the majority were male (70.8%) and Caucasian (92.7%), with a median (IQR) age of 53.3 (47.5-59.0) years, BMI of 26.2 (23.2-29.5), and MELD of 15 (13-19). 94.6% of recipients received a right lobe graft and 70.8% of recipients were biologically related to their donor. Compared with recipients who underwent LDLT for other etiologies of liver disease, those with ALD had a greater proportion of male recipients (70.8% vs. 55.9%, p<0.001) and concomitant HCV diagnosis (44.6% vs. 36.6%, p=0.048). ALD recipients were significantly older (53vs.52years, p=0.02) with a greater weight (79.2vs.75.0 kg, p=0.04). There was no difference in median BMI or MELD. Post-operatively, there was no significant difference in median number of complications between ALD vs. non-ALD (3 vs. 3, p=0.75), nor was there a difference in highest Clavien grade (2 vs. 2, p=0.23). Patient survival was similar for ALD and non-ALD recipients at one (94% vs. 91%), five (83% vs. 79%), and ten (61% vs. 66%) years post-transplant (p=0.32) (Figure 1). Similarly, no significant differences were detected in graft survival between ALD and non-ALD recipients at one (88% vs. 84%), five (76% vs. 74%), or ten (55% vs. 61%) years post-transplant (p=0.29).

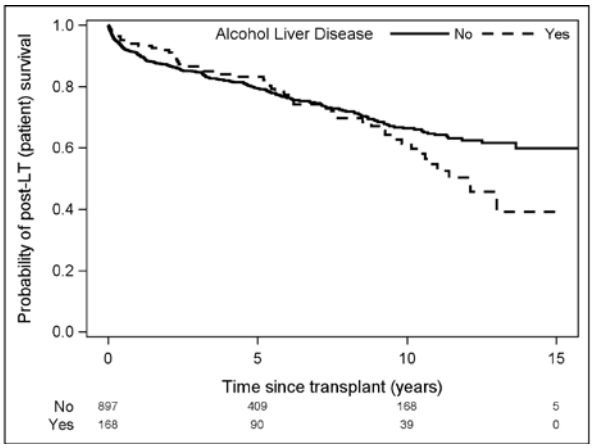

Figure 1: Patient survival among recipients transplanted for ALD and those transplanted for other etiologies of liver disease.

Conclusions: Though there were early concerns regarding recipient outcome and potential recidivism, ALD is now a well-recognized indication for liver transplantation. While we do not have data regarding pre-transplant abstinence and post-transplant recidivism in the A2ALL cohort, we found no significant difference in major complications, patient survival, or graft survival among patients transplanted for ALD and those transplanted for other etiologies of liver disease. These findings suggest LDLT is a safe and successful option for patients who require liver transplantation for ALD.

Developing a Murine Model to Study Novel Therapies for Tolerance in Vascular Composite Tissue Allotransplantation

Conkling, Nicole; Kaul, Anupurna; Nguyen, Vinh; Tang, Qizhi

Introduction: The field of vascularized composite tissue allotransplantation (VCTA) still faces many clinical challenges in the prevention and treatment of graft rejection. Episodes of acute and chronic rejection occur nearly universally in VCTA, requiring elevated doses of toxic immunosuppression, and resulting in increased morbidity for both graft and patient [1-3]. Cellular therapies are of particular interest to VCTA researchers, including the adoptive transfer of tolerogenic T-regulatory cells (Tregs) [4]. The concurrent application of chimeric antigen receptor (CAR) technology to Tregs aims to improve their potency and donor-specificity, potentially enhancing their graft-protective effect without resulting in global host immunosuppression [5]. By utilizing a transgenic donor C57BL/6 (B6) mouse that expresses HLA-A2, our CAR target molecule, in our transplant model, we aim to characterize the kinetics and characteristics of graft rejection in a single-allele mismatched donor-recipient pair, with the ultimate goal of transferring our engineered Tregs to treat or prevent rejection.

Methods: To first describe the rejection kinetics of non-vascularized transplants of low antigenic load, we performed skin transplants between A2-positive donor B6 mice and wild-type B6 recipients. The skin grafts were monitored for initial engraftment, and subsequently followed for timing of rejection. In a second cohort of mice (n=2), A2-positive kidney capsule islet transplants (300 mouse islets) were performed in STZ-induced diabetic B6 recipients. Graft take, and subsequent rejection, was monitored with daily blood glucose measurement (mg/dL).

It is important for our murine model to account for the differences in timmunogenicity of the multiple types transferred in VCTA. While skin has been described to be the most immunogenic, it represents only a component of the challenges in improving immune tolerance of the allograft. Hindlimb transplant involves the vascularized connection of the femoral artery and vein of the donor and recipient utilizing a microsurgical cuff technique, illustrated in Figure 1 [6]. The femur is fixated using a spinal needle as an intramedullary nail, and the thigh muscles and skin are repaired. Perfusion is monitored clinically during the immediate postoperative period to ensure graft success. Initially, syngeneic transplants will be performed to validate technique before application in the single-allele mismatch pair.

Results: All initial skin grafts (n=5) survived initial engraftment. By day 10, the single-allele mismatch skin transplants showed signs of acute rejection, and the grafts were completely rejected by day 14 post-transplant. Islet transplants (n=2) were similarly initially successful by blood glucose monitoring; however, for the duration of the study, the islet grafts were not rejected (Figure 2).

Other investigators with experience in murine hindlimb transplant show acute rejection at 7 days in a fully allogenic model (BALB/c to B6), as compared to syngeneic grafts, which are tolerated indefinitely [7]. Once this model is reliably established in our hands, we expect to see slower rejection kinetics in single-allele mismatch.

Conclusions and future directions: Non-vascularized transplant models of low antigenic load, such as skin and islet transplant, offer different perspectives on the kinetics of single-allele mismatch rejection. While skin is an extremely stringent model for rejection, it is believed to be the most immunogenic component of the vascularized composite graft. Our results from islet transplant, however, suggest that the A2 allele may not be a potent enough antigen to result in florid acute rejection. The mouse hindlimb surgical model is technically demanding; however, once we characterize the rejection process in single-allele mismatch VCTA, we will be able to better identify the potential benefits, or possible off-target or graft effects, of our HLA-A2-specific CAR.

References:

1. Sarhane, K.A., et al., *A critical analysis of rejection in vascularized composite allotransplantation: clinical, cellular and molecular aspects, current challenges, and novel concepts.* Front Immunol, 2013. **4**: p. 406.
2. Mundinger, G.S. and C.B. Drachenberg, *Chronic rejection in vascularized composite allografts.* Curr Opin Organ Transplant, 2014. **19**(3): p. 309-14.
3. Fischer, S., et al., *Acute rejection in vascularized composite allotransplantation.* Curr Opin Organ Transplant, 2014. **19**(6): p. 531-44.
4. Fryer, M., et al., *Exploring cell-based tolerance strategies for hand and face transplantation.* Expert Rev Clin Immunol, 2015. **11**(11): p. 1189-204.
5. Boardman, D., et al., *Antigen-specificity using chimeric antigen receptors: the future of regulatory T-cell therapy?* Biochem Soc Trans, 2016. **44**(2): p. 342-8.
6. Sucher, R., et al., *Mouse hind limb transplantation: a new composite tissue allotransplantation model using nonsuture supermicrosurgery.* Transplantation, 2010. **90**(12): p. 1374-80.
7. Furtmuller, G.J., et al., *Orthotopic Hind Limb Transplantation in the Mouse.* J Vis Exp, 2016(108): p. 53483.

Figure 1:

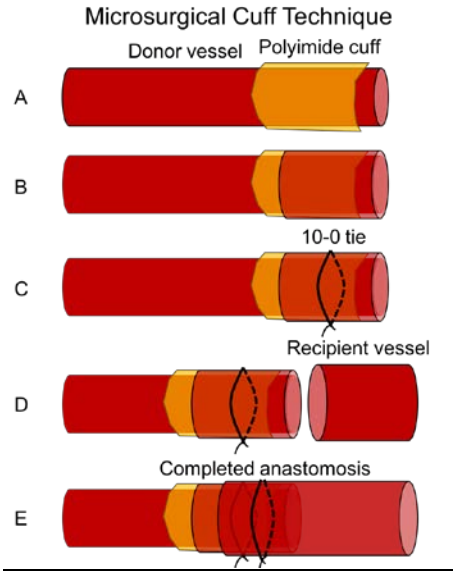

Figure 2:

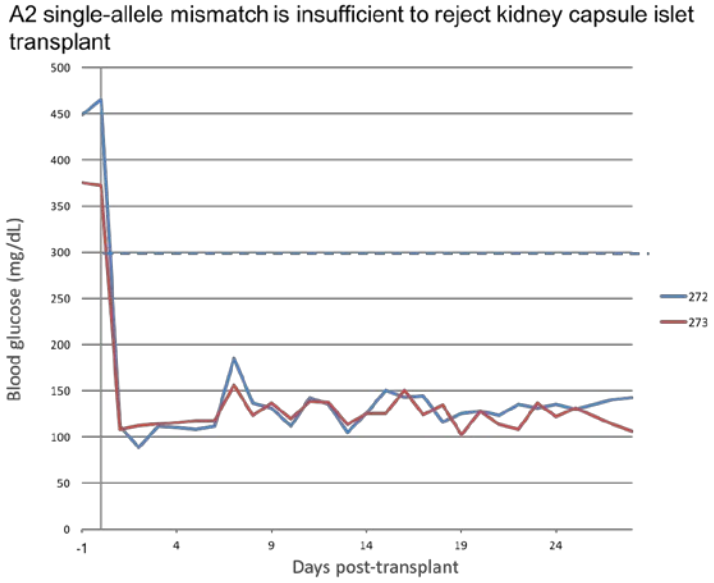

Active Surveillance Versus Immediate Resection for Non-Functioning Pancreatic Neuroendocrine Tumors: a cost-effectiveness analysis

Kathryn H Chomsky-Higgins, MD, MS[1,2], Carolyn D Seib, MD, MAS[1], Iheoma Nwaogu, MD[1], Yufei Chen, MD[1], Jessica E Gosnell, MD[1], Wen T Shen, MD, MA[1], Quan-Yang Duh, MD[1], Insoo Suh, MD[1]

[1]Endocrine Surgery, University of California, San Francisco, [2]General Surgery, UCSF East Bay General Surgery

Introduction

Small, non-functioning pancreatic neuroendocrine tumors (NF-PNETs) are increasingly prevalent and present a vexing challenge for providers. Data representing true risk of malignancy are conflicting, and the procedures required to resect such tumors are costly and morbid. Consideration of an active surveillance approach to non-functional PNETs less than 2cm in size has been advocated by both the European Neuroendocrine Tumor Society and the National Comprehensive Cancer Network. No cost-effectiveness analysis has been performed to rigorously evaluate the relative merits of these strategies given currently available data.

Methods

We constructed a decision-analytic model to evaluate surgical and active surveillance management strategies for small (<2cm), sporadic, asymptomatic, NF-PNETs. Costs, utility values, and transition probabilities were identified by literature review. The model used a healthcare system perspective, global 3% standard discounting, and a lifetime time horizon. We tested a strategy of immediate surgery after diagnosis versus an active surveillance strategy. Threshold and sensitivity analyses on key parameters were conducted to assess robustness of the model. Costs were represented in 2018 US dollars, and health outcomes were represented in quality-adjusted life-years (QALYs).

Results

In the base case, the model predicted a preferred strategy of immediate surgery, with an incremental cost-effectiveness ratio (ICER) of $9269/QALY. The model was sensitive to the mortality hazard ratio attributed to a strategy of active surveillance with a threshold of 0.55. While surgical mortality and cost also had a notable impact on the model, their influence was not sufficient to suggest a change in optimal strategy. The model was robust to sensitivity analysis of remaining inputs, including cost of surveillance, probability of progression to requiring surgery while under active surveillance, and accuracy of active surveillance testing.

Conclusions

To our knowledge, this is the first cost-utility analysis evaluating management strategies for small, sporadic, asymptomatic, NF-PNETs. Data informing our understanding of the increased mortality attributable to an active surveillance strategy, reflecting malignancy risk in these tumors, are contradictory. Our model suggests that until we can draw more definitive conclusions with respect to underlying malignancy risk in small NF-PNETs, the safest and most cost-effective management strategy is surgical resection.

Tumor Infiltrating Lymphocyte Directed Neoadjuvant Therapy in Operable Stage III Melanoma

Kelly M Mahuron, Priscila Munoz Sandoval, Margaret Lowe, Mariela Pauli, Evan Henley, Katy Tsai, Alain Algazi, Adil Daud, Michael Rosenblum, Michael Alvarado

Introduction:

We have previously demonstrated that the frequency of tumor infiltrating lymphocytes that express both the inhibitory proteins PD-1 and CTLA-4 (peTILs) predicts response to anti–PD-1 monotherapy as well as combination CTLA-4/PD-1 blockade in patients with metastatic melanoma. However, the utility of this assay has not been established in the neoadjuvant setting. Patients with operable stage III melanoma have a high rate of recurrence after surgery and adjuvant systemic therapy, and the role of neoadjuvant therapy in these patients is currently undefined. Also, treatment with immunotherapy is often limited in patients due to its adverse autoimmune side effects. In this study, seven patients with operable stage III melanoma were assessed for response to neoadjuvant anti-PD-1 or anti-PD-1/CTLA-4 therapy assigned by peTIL frequency.

Methods:

Pretreatment tumor samples from seven patients with locally advanced melanoma underwent flow cytometric analysis. Patients with high peTILs (>20%) received neoadjuvant anti–PD-1 monotherapy, and patients with low peTILs (<20%) received anti-PD-1/CTLA-4 combination therapy. All patients then underwent surgical resection. Patients with documented follow up history and evaluable immunophenotypes were included in efficacy and safety analysis.

Results:

Patients were 57% male with a mean age of 58 years. All seven patients had either stage IIIB or IIIC disease, and five patients had BRAF wild-type tumors. Prior therapy included CTLA-4 monotherapy in two of seven patients. Five patients received anti-PD-1 monotherapy, and two patients received CTLA-4/PD-1 combination blockade. Six out of seven patients achieved a complete pathologic response. Responses were durable, and at a median follow-up of 21 months only the patient who did not achieve a complete pathologic response had disease progression. Toxicity profiles were minimal and consistent with previously reported studies with grade 1/2 diarrhea and hypothyroidism most frequently reported.

Conclusions:

Our study supports the efficacy of peTIL directed neoadjuvant treatment in operable Stage III melanoma with the large predominance of patients achieving complete pathologic response with acceptable toxicity profiles. This promising data from our pilot study merits further investigation with a larger cohort validation study or a clinical trial.

An Improved Method of Minimally Invasive Pulmonary Metastasectomy that Allows Full Palpation of the Lung Without Chest Wall Disruption

Greg J. Haro, Joseph A. Reza, Amanda Sammann, Kirk D. Jones, David M. Jablons and Michael J. Mann

Introduction

The technical approach to surgical pulmonary metastasectomy is controversial. Conventional video-assisted thoracic surgery (conVATS) does not allow the palpation of the lung that is possible via open thoracotomy (Open), resulting in missed lesions that had been identified on pre-operative imaging and a failure to identify occult lesions. We developed a modified VATS technique (modVATS) that allows direct palpation of the entire lung similar to Open, while maintaining a minimally invasive approach. In this retrospective observational study, we report our experience with pulmonary metastasectomy by modVATS, conVATS, and Open.

Methods

We identified 444 patients with pulmonary metastasis (sarcoma n=192, non-sarcoma n=252) who underwent 556 pulmonary metastasectomies by modVATS (n=92), conVATS (n=162), and Open (n=302) with the intention of complete oncologic resection at UCSF Medical Center between 1991 and 2015. We reviewed preoperative imaging, operative, and pathology reports to identify the sizes and locations of all lesions. Data were analyzed with Student's t-test, Pearson's chi-squared test, Fisher's exact test, Kaplan-Meier survival estimate with log-rank and Wilcoxon tests, and logistic regression.

Results

94% of metastasectomies were complete oncologic resection. Lesions were missed in 11% of conVATS, 5% of Open, and 3% of modVATS ($P<0.05$, conVATS vs. Open or modVATS). Conversely, new lesions not seen on preoperative imaging were resected in 41% of Open and 45% of modVATS, but only in 25% of conVATS ($P<0.01$, conVATS vs. Open or modVATS). These new lesions were <2mm in 59% of modVATS, 12% of conVATS, and 16% of Open. Mean total discrepancy of number of new lesions to missed lesions resected was 1.1 in modVATS, 0.8 in Open, and 0.2 in conVATS ($P<0.01$, conVATS vs. Open or modVATS).

Patients were followed for a mean of 4.1 years and a median of 2.8 years (range 0.02-19.6), and the entire cohort had a 5-year overall survival of 41%. Survival of sarcoma patients was significantly worse than that of metastasectomy patient with other forms of cancer ($P=0.01$); sarcoma comprised a significantly higher percentage of modVATS vs conVATS (90% vs. 23%, $P<0.01$). Among patients who experienced recurrence, recurrence ipsilateral to the side of a previous metastasectomy occurred in 55% of modVATS, 69% of Open, and 81% of conVATS ($P<0.01$, modVATS vs. conVATS). After adjustment for age, sex, diagnosis, disease free interval, and presence of extra-pulmonary metastasis, modVATS had 0.4 the odds of ipsilateral recurrence in comparison to conVATS (95% CI 0.1-0.98) and no difference in comparison to Open. There was no difference in overall recurrence or survival for the entire cohort, but given the substantially higher proportion of sarcoma patients in the modVATS vs. conVATS groups, a separate analysis was performed only among sarcoma patients whose survival had been demonstrably worse. Median survival for sarcoma patients with pulmonary metastasis was significantly better in modVATS patients compared to Open (3.5 vs. 2.7 years, $P=0.004$), and despite the small sample of conVATS sarcoma patients (n=36) a trend to improved survival in modVATS vs. conVATS was also observed (3.5 vs. 2.7, $P=0.16$).

Conclusions

modVATS is a novel minimally invasive technique with technical and clinical outcomes that are improved compared to conVATS. This approach yielded results that were at least as good as open surgery, while continuing to optimize recovery and possibly allow a more widespread application of aggressive surgical and multimodality clinical strategies, particularly for sarcoma.

Summary of Technical and Clinical Outcomes

Outcome	modVATS n = 92	conVATS n = 162	Open n = 302	modVATS vs conVATS *p* Value	modVATS vs Open *p* Value	conVATS vs Open *p* Value
Missed Lesion Y/N	3 (3.3)	18 (11.1)	15 (5.0)	0.03	NS	0.01
# Missed Lesions +/- SD	1 +/- 0	1.2 +/- 0.6	2.1 +/- 1.5	NS	NS	0.02
New Lesion Y/N	41 (44.6)	41 (25.3)	125 (41.4)	<0.01	NS	<0.01
New Lesion <2mm Y/N	24 (58.5)	5 (12.2)	20 (16.0)	<0.01	<0.01	NS
# New Lesions +/- SD	2.6 +/- 2.9	1.3 +/- 0.9	2.2 +/- 1.9	0.01	NS	<0.01
Mean Total Discrepancy +/- SD	1.1 +/- 2.3	0.2 +/- 0.9	0.8 +/- 1.8	<0.01	NS	<0.01
Overall Recurrence Y/N	64 (69.6)	72 (44.4)	176 (58.3)	<0.01	0.05	<0.01
Ipsilateral Recurrence Y/N	35 (54.7)	58 (80.6)	122 (69.3)	<0.01	0.04	0.07
Median Survival Years (95% CI)	3.8 (3.0-5.4)	3.9 (2.9-5.3)	3.1 (2.2-4.0)	NS	NS	NS
Sarcoma	3.5 (2.9-5.4)	2.7 (1.1-5.5)	2.2 (1.6-2.7)	0.16	<0.01	NS

Mechanisms of Facial Fracture in the Homeless at an Urban Level I Trauma Center

Audrey Nguyen MD, Barbara Grimes PhD, John Neuhaus PhD, Jason Pomerantz MD

Background: Homeless patients are a vulnerable group who are susceptible to traumatic injuries, including facial fractures. However, little is known about the characteristics or risk factors for facial fractures among homeless patients. In patients with facial fractures, we investigated the association between homelessness and the mechanism of injury and type of facial fracture.

Methods: We conducted a retrospective study of 2,221 adult trauma patients who sustained facial fractures and were treated at Zuckerberg San Francisco General Hospital from 2011 to 2016. Demographic and clinical data were recorded in a standardized registry of trauma patients. We used a two-sided t-test and univariate and multivariate logistic regression to evaluate the association between homelessness and mechanism of injury and facial fracture type.

Results: Among patients with facial fractures, 12% were homeless. Compared to housed patients, homeless patients were more likely to be male, black, and test positive for drug use (all $p<0.0001$). The homeless patients were less injured, but had longer hospital stays and were more likely to be discharged to the community than a rehabilitation facility (all $p<0.0001$). Homeless patients were more likely to have a mandible fracture ($p=0.0140$) and more likely to need surgery for their facial fractures (12.7% vs. 7.8%, $p=0.0090$) compared to housed patients. Mandible surgery was the most common type of facial surgery in both groups with higher rates in the homeless group (7.6% vs. 3.4 %, $p=0.009$). After adjusting for age, gender, race, drug and alcohol use, and co-morbid conditions, homeless patients with facial fractures were over 2x more likely to have been assaulted (OR2.4, 95% CI 1.63 – 3.51).

Conclusions: Homeless patients with facial fractures are more likely to have been assaulted, suffer mandible fractures, and require surgery for their facial fractures. Further investigations of these unique characteristics in this at-risk population can help guide identification, treatment, and prevention efforts to reduce the incidence of facial fractures and improve outcomes for homeless patients.

	Homeless (n=275)	**Housed (n=1946)**	***p*-value**
Age in years, mean	45 ±12	48 ± 21	0.2700
Male, percent	250 (91%)	1464 (75%)	<0.0001
Race, percent □ White □ Black □ Asian □ Other/Unknown	 185 (67%) 61 (22%) 7 (3%) 22 (8%)	 1323 (68%) 217 (11%) 315 (16%) 91 (5%)	<0.0001
ISS, mean	12±10	14±12	<0.0001
Assault, percent	129 (47%)	423 (22%)	<0.0001
Positive urine drug test, percent	80 (29%)	153 (8%)	<0.0001
Length of Stay, mean (days)	8.6±17.1	6.0±13.3	<0.0001
Discharged to community, percent	150 (55%)	867 (45%)	<0.0001
Mandible fracture, percent	38 (14%)	155 (8%)	0.0140
Surgery for facial fracture, percent	35 (13%)	152 (8%)	0.0092
Mandible surgery, percent	21 (8%)	67 (3%)	0.0092

The Impact of Pro-Inflammatory States on the Fibrin-Platelet Balance Following Injury

Authors: Anamaria J. Robles, Lucy Z. Kornblith, Amanda S. Conroy, Mitchell J. Cohen, Rachael A. Callcut

BACKGROUND: In non-injured patients, aging and HIV infection are both known to induce chronic pro-inflammatory milieus with associated hypercoagulable states. Studies have demonstrated that both elderly patients and HIV patients have increases in pro-coagulant factors and decreases in anti-coagulant factors. Although antiretroviral therapy (ART) decreases viral replication for the HIV patients, low-level inflammation and immune activation are known to persist. Overall, the impact of the pro-inflammatory states of aging (≥55 years) and HIV infection on post-injury coagulation is unknown. We hypothesized that these patients demonstrate hypercoagulable states following even severe injury.

METHODS: Data were prospectively collected on 1671 injured patients from 2005-2016. Citrated rapid thromboelastography (CRT), functional fibrinogen levels (FLEV), and standard coagulation measures were performed. Patients on anti-coagulant/anti-platelet medications were excluded from analysis. Multiple regression analysis was performed to determine the independent associations of age and HIV infection on coagulation.

RESULTS :
Amongst 1671 patients enrolled, 22% were age ≥55 years and 39 (3%) were HIV positive amongst the 1349 in whom their HIV status was known. Older patients were more severely injured (ISS 21 vs 12) and had lower hemoglobin (13 vs 14 g/dL) and platelet counts (231 vs 275 k/uL; all $p<0.01$) compared to their younger counterparts. 18 of the HIV patients (46%) were on ART, with 24 (69%) having history of ART treatment; the median CD4 count was 399 (227-536 cells/mm3). HIV infected patients trended towards being older (43 vs 37 years, p=0.05) and had significantly lower BMI (24 vs 26 kg/m2 p<0.01) compared with HIV-negative patients. They also had lower hemoglobin (13 vs 14 g/dL, p<0.01), platelet counts (239 vs 269 103/µL, p<0.01), and WBC (7.8 vs 9.8 103/µL, p=0.01). In multiple logistic regression, older patients were hypercoagulable with *increased* speed of clot formation (CRT alpha angle +2.34°, $p=0.03$), *increased* levels of functional fibrinogen (FF FLEV +45.57mg/dL, $p=0.01$), but *lower* platelet contributions to clot strength (-3.80%, $p<0.01$). Similarly, in multiple logistic regression HIV infected patients were also hypercoagulable with increased speed of clot formation (CRT alpha angle +4.90°, p=0.02). However, in contrast to the older cohort, they had decreased levels of functional fibrinogen (FF FLEV -67.30 mg/dL, p=0.04), and higher platelet contributions to clot strength (+9.03%, p=0.02).

Age ≥ 55 years	**Mean Difference**	**SE**	***p*-value**
CRT R-time (min)	-0.10	0.13	0.44
CRT K-time (min)	-0.21	0.17	0.23
CRT alpha angle (°)	2.34	1.07	**0.03**
CRT MA (mm)	1.29	1.26	0.31
CRT ly30 (%)	-1.94	1.02	0.06
FF FLEV (mg/dL)	45.57	18.32	**0.01**
Plt contribution to clot strength (%)	-3.80	1.30	**<0.01**
HIV	**Mean Difference**	**SE**	***p*-value**
CRT R-time (min)	-0.22	0.27	0.42
CRT K-time (min)	-0.55	0.38	0.14
CRT alpha angle (°)	4.90	2.11	**0.02**
CRT MA (mm)	0.11	2.65	0.97
CRT ly30 (%)	0.29	1.14	0.80
FF FLEV (mg/dL)	-67.30	32.67	**0.04**
Plt contribution to clot strength (%)	9.03	3.97	**0.02**
Anti-thrombin III (% activity)	-17.64	8.85	**0.04**

CONCLUSION: Following injury, pro-inflammatory states including aging and HIV infection have independent associations with hypercoagulability and alterations in the fibrin-platelet balance. Identifying fibrin-platelet imbalances following injury is critical, as targeted treatment may require shifts in resuscitation and thromboprophylaxis in at-risk populations including those with chronic pro-inflammatory states.

Cost Burden of Overtreating Low Grade Pancreatic Cystic Neoplasms

Sharib J, Wimmer K, Fonseca A, Shen Y, Koay E, Maitra A, Esserman L, Ozanne E, Kirkwood K

Introduction: Prevalence of intraductal papillary mucinous neoplasm (IPMN) is increasing dramatically. International consensus guidelines (ICG) recommend resection of IPMN with high risk stigmata, and laborious surveillance for cysts with worrisome features. In practice, resections are performed at higher rates due to fear of malignancy. As a result, many cysts harboring no or low grade dysplasia (LGD) are removed unnecessarily, with undue risk to patients. We utilize a cost-effectiveness model to define the burden of overtreating pancreatic cysts and determine the accuracy required for the benefits of diagnostic modalities to outweigh risks.

Methods: We used a Markov decision model to calculate the cost-effectiveness of three treatment strategies for IPMN; "Surgery" for all, Do-nothing, or "Surveillance" based on ICG. To estimate the cost-burden of resecting LGD, a "Precision Surveillance" strategy was created that eliminated the possibility of resecting LGD in surveillance. Survival was estimated by a microsimulation time series. To define the minimum accuracy required for a diagnostic, a sensitivity analysis, which considered all possible values of diagnostic sensitivity and specificity for Surveillance, evaluated the incremental cost-effectiveness ratio (ICER) of Surveillance compared to the other strategies. A strategy was cost-effective if the ICER was <$100,000 above the index strategy (Do-nothing).

Results: Surveillance increases costs $64,103/QALY compared to Do-nothing for the base-case. Precision Surveillance results in an incremental cost *discount* of $19,338/QALY compared to current Surveillance, making it the preferred strategy overall. Survival in years 1 to 5 for both Surgery and Surveillance are worse compared to Do-nothing. While, Precision Surveillance improves survival compared to current all strategies. When plotting the ICER for each strategy against sensitivity, Surveillance is always cost-effective compared to Do-nothing, but only dominates Surgery when sensitivity is >64%, which is achieved currently (Figure 1a). Specificity is more influential (Figure 1b). Below 34% specificity, Do-nothing is the favored strategy. Between 34% and 51% no strategy is favored. Surveillance is clearly favored for specificity >51%, however, current ICG achieve only 27-45% specificity.

Conclusion: Our present inability to distinguish low grade from high grade/invasive lesions adds significant costs and early mortality to the treatment of IPMN. Improved diagnostics that accurately grade cystic pancreatic neoplasms and empower clinicians to reduce the resection of LGD would decrease overall costs and improve effectiveness and survival of surveillance.

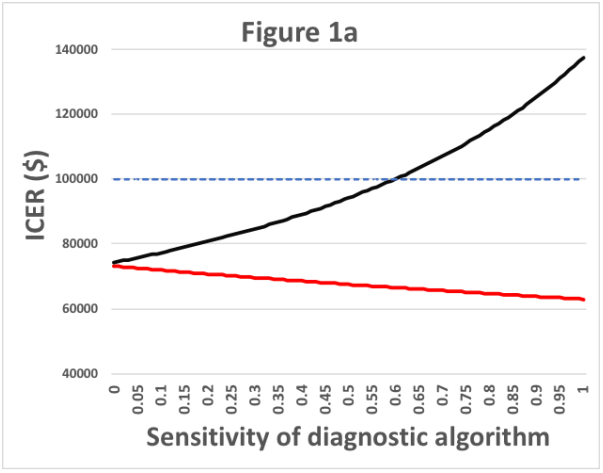

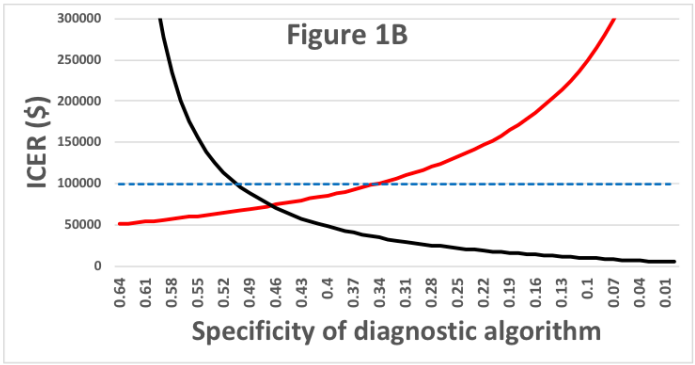

Figure 1: Comparative cost-effective of Do Nothing vs Surveillance (red lines) and Surgery for all vs Surveillance (black lines) over all possibilities of sensitivity (A) and specificity (B) of a diagnostic management algorithm. Dotted blue line marks the $100,000 societal willingness to pay threshold for improvement of one QALY (ICER).

Tissue-Factor Targeted Nanoparticles for the Prevention of Neointimal Hyperplasia Following Vascular Intervention

Evan Werlin, Elizabeth Levy, Thomas Sorrentino, Mian Chen, Bian Wu, Melinda Schaller, Tejal A Desai, Michael S Conte

Introduction: The long-term success of interventions for peripheral arterial disease is limited by restenosis due to intimal hyperplasia, which we believe is caused by an aberrant, persistent inflammatory response. Specialized pro-resolving lipid mediators (SPM) such as resolvin D1 (RvD1), have been shown to counteract inflammation and promote the process of resolution. We investigate the use of a novel, targeted, biodegradable nanoparticles (NP) for the delivery of RvD1 following vascular intervention.

Methods: NP were prepared from poly(lactic-*co*-glycolic acid) (PLGA) co-polymers across a variety of lactic acid: glycolic acid (L:G) ratios using a single emulsion technique. NP were loaded with RvD1 and assessed for maximal loading and release across a variety of L:G ratios. Peptides targeted to Tissue Factor (TF) or non-specific (nonsense) peptides were conjugated to the surface of the NP with a FITC fluorophore using malamide thiol chemistry. TF-targeted and nonsense-NP across a range of concentrations (1 nM – 100 nM equivalent RvD1 loading) were then incubated in microplate wells coated with recombinant TF (500 ng/well) to assess targeted binding.

Results: 75:25 (L:G) PLGA NP demonstrated increased RvD1 loading (507.3 ± 42.8 pg RvD1/mg PLGA) as compared to 50:50 (L:G) (121.5 ± 14.2 pg RvD1/mg PLGA), 85:15 (143.8 ± 2.2 pg RvD1/mg PLGA) and 100:0 (L:G) (200.1 ± 18.6 pg RvD1/mg PLGA) PLGAs. 75:25 (L:G) PLGA NP also demonstrated increased RvD1 release after 5 days (153.2 ±19.8 pg RvD1/mg PLGA) as compared to 50:50 (L:G) (50.8 ± 9.3 pg RvD1/mg PLGA), 85:15 (22.1 ± 1.6 pg RvD1/mg PLGA) and 100:0 (L:G) (38.6 ± 9.6 pg RvD1/mg PLGA) PLGAs. Targeted-NP showed increased binding to TF-coated wells as compared to nonsense-NP at 100 nM (35.7±1.6 v. 23.5±0.7; $p<0.001$) and 50 nM (41.6±0.9 v. 32.7±0.6; $p<0.001$) NP concentrations (Figure 1).

Conclusions: 75:25 (L:G) PLGA NPs provide an attractive means of RvD1 delivery to both vein grafts and arteries following angioplasty. TF-targeted NP demonstrated effective binding to recombinant TF and offer great potential for delivery of RvD1 in a rat model of carotid angioplasty. Moving forward, our lab will continue with the characterization of these targeted particles and load them with RvD1 for use in our animal model assessing for acute markers of inflammation as well as its effects on neointimal hyperplasia.

Figure 1: TF-targeted NP demonstrate increased binding to TF-coated wells (500 ng/well) across a range of NP concentrations.

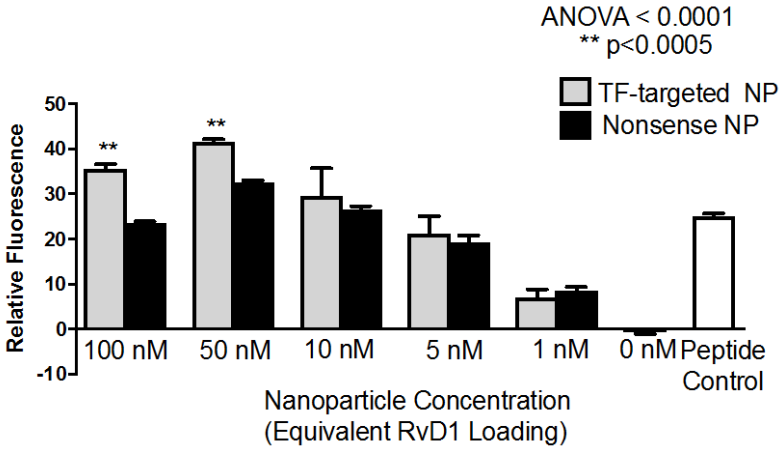

The *Ex Vivo* Perfused Human Lung as a Model of Acute Lung Injury in Sepsis

James T. Ross, Nicolas N. Nesseler, Jeffrey E. Gotts, Michael A. Matthay

Introduction: Acute lung injury in sepsis is a common complication that likely reflects the impact of both systemic inflammation and bacteremia. Injury involves vascular endothelial injury and the loss of alveolar epithelial barrier function, including increased permeability to protein, and a decrease in alveolar fluid clearance (AFC). The time-course of injury and relative contribution of these factors is incompletely understood. The *ex vivo* perfused human lung allows us to test the mechanisms of acute lung injury without the confounding effects of other organs. The goal in these studies was to evaluate the time-course of epithelial and endothelial injury in the *ex vivo* lung when exposed to *S. pneumoniae.*

Methods: Human lungs rejected for transplant were received from Donor West. The right or left lung was selected based on gross appearance, and the pulmonary artery and main bronchus were cannulated. A 3 Fr catheter was passed through the main bronchus into the distal airspaces to sample alveolar fluid. The lung was perfused with DME-H21 and 5% BSA at 37°C to maintain a PA pressure of 10 cmH_2O. Perfusate drained passively from the pulmonary veins and collected in a reservoir at the base of the chamber. When the temperature of the venous drainage reached 37°C, the lungs were inflated with room air at a continuous positive airway pressure of 8 cmH_2O. 100ml of fresh human blood was added to the perfusate and, in half of the lungs, approximately 10^{10} *S. pneumonia* were added to the perfusate. The alveolar space and perfusate were sampled every hour for biomarker analysis. AFC was measured at 0 and 5 hours by instilling 100ml of 5% albumin into the distal airspaces and comparing the total protein concentration of the air space fluid at 5 and 35 minutes. Endothelial and epithelial permeability were evaluated by measuring the accumulation of IgM from the perfusate in the airspaces.

Results: In this pilot study of 12 lungs, the majority (83%) had normal AFC at 0 and 5 hours. Lungs with an abnormal starting AFC (<10%) were excluded from further analysis. The average weight gain was 78% (range 43-267%). The addition of *S. pneumoniae* was not associated with a significant change in AFC or weight gain.

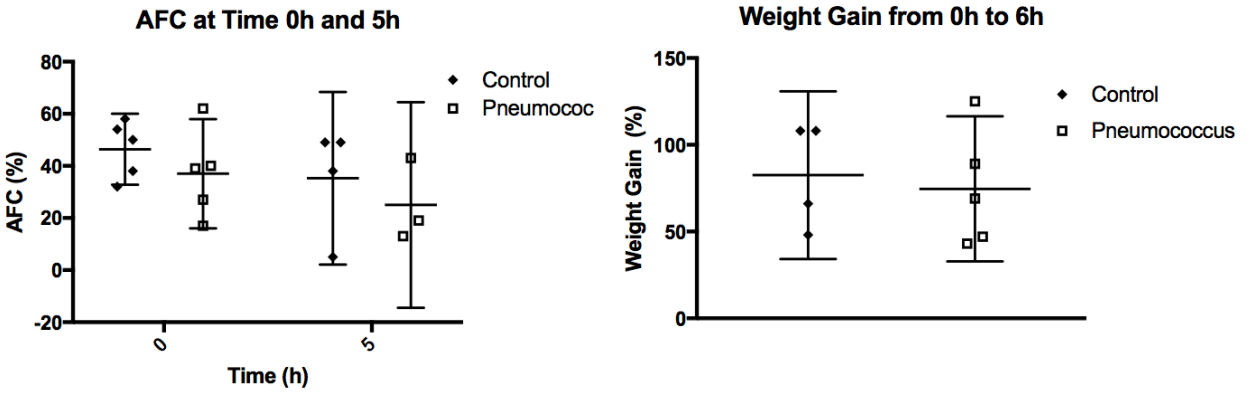

Conclusions/Next Steps: The initial results suggest that many lungs rejected for transplant have a normal fluid clearance across the alveolar epithelium, and that AFC can be maintained for at least six hours in our *ex vivo* preparation. Further, alveolar epithelial function appears to be resistant to damage from iv S. pneumonia. Measurement of IgM accumulation in the airspaces will allow us to distinguish whether the observed weight gain reflects exclusively endothelial injury or a combination of endothelial and epithelial injury. Future biomarker analysis will allow a more detailed study of the pattern of injury.

Hyponatremia and Complex Biliary Disease

Michael Zobel, MD and Lygia Stewart, MD

Introduction: Our goal was to determine whether there was a direct correlation between serum sodium and the severity of illness among patients presenting with gallstone disease. Low serum sodium has previously been described in the context of other intra-abdominal infectious and inflammatory conditions.

Methods: Multivariate analysis of 830 patients with gallstone disease (724 men, 106 women; average age 62) treated at the San Francisco VA Medical Center and an affiliated academic medical center, from March 1989 to December 2017. Minimum serum sodium within 24 hours of presentation, prior to intervention, was collected for each patient. Charlson comorbidity index (CCI) was calculated. Gallstones, bile, and blood (as clinically relevant) were cultured. Illness severity was characterized for each patient: 1) none (no infectious manifestations), 2) systemic inflammatory response syndrome, 3) severe (gangrenous cholecystitis, cholangitis, necrotizing pancreatitis, etc.), or 4) multiple organ dysfunction syndrome (bacteremia, hypotension, organ failure).Pathology, when available, was reviewed.

Results: True hyponatremia (Na <135 mEq/L) was present in 229 cases (28%). On bivariate analysis, decreased serum sodium was significantly associated with worsening illness severity, ascending bacterial infection, gangrenous changes, elevated CCI score, increasing age, and serum glucose. On multivariate analysis, all factors (except age and serum glucose) independently correlated with serum sodium and factors were additive. Figure 1 below demonstrates the statistically significant inverse association between serum sodium and disease severity, while also accounting for comorbid state. Figure 2 demonstrates a similar relationship with a higher level of bacterial infection and the presence of gangrene.

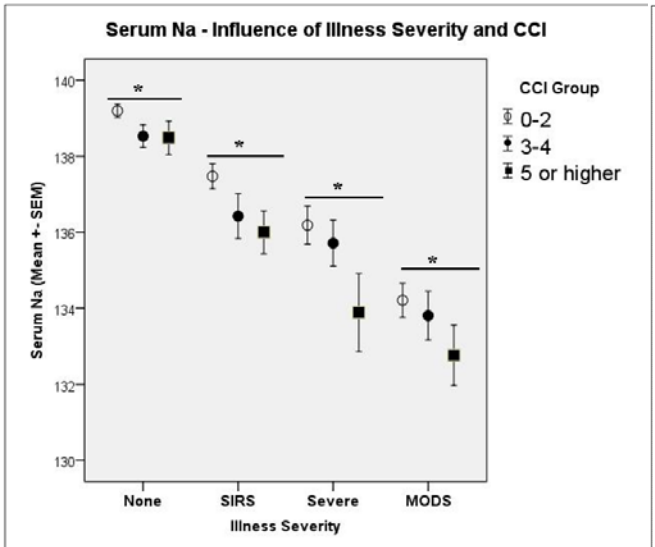

Figure 1. Illness severity and Charlson Comorbidity Index score are both independent predictors of serum sodium. P values significant (<0.0001) for all.

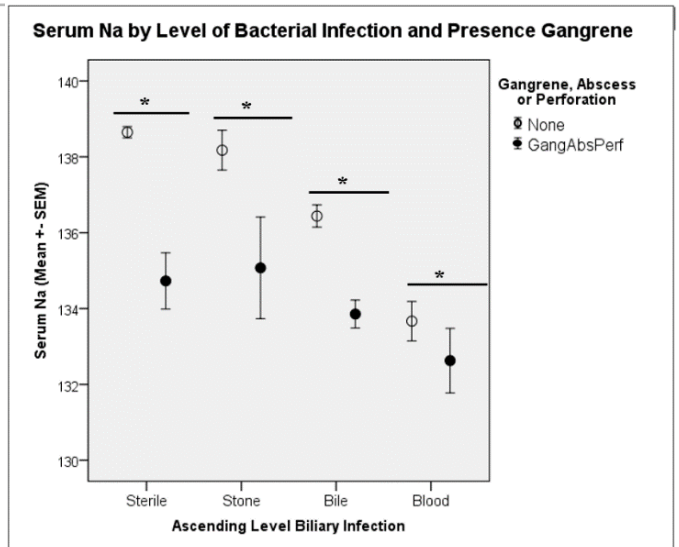

Figure 2. Higher level of biliary infection and the presence of gangrene are both independent predictors of serum sodium. P values significant (<0.02) for all pairings.

Conclusion: Our study illustrates an inverse, independent correlation between illness severity and serum sodium. Culture data demonstrated serum sodium predictably decreased as bacterial infection ascended from gallstone colonization to bactibilia to bacteremia. Patient comorbidity and the presence of gangrenous changes also independently correlated with decreased serum sodium on multivariate analysis.

Optimization and Validation of the EconomicClusters Model for Facilitating Health Disparities Research in Low-Resource Settings

Lauren Eyler, Alan Hubbard, Catherine Juillard

Introduction: Health disparities research in low- and middle-income countries (LMICs) is hampered by the difficulty of measuring patient economic status in low-resource settings. We had previously developed the EconomicClusters k-medoids clustering-based algorithm for defining population-specific economic models based on few Demographic and Health Surveys (DHS) assets and now aimed to optimize and validate this model.

Methods: We used agglomerative hierarchical clustering to simplify the twenty-group economic model we had previously developed for Cameroon into fewer, ordinally ranked groups based on three correlates of socioeconomic status: mean cluster child height-for-age Z-score (HAZ, a marker of nutritional status), women's literacy score, and proportion of children who are deceased. We modified the EconomicClusters algorithm to allow an option for researchers to select the minimum number of clusters that meets a defined threshold of our optimization criterion (the average silhouette width, ASW) in order to create models with fewer clusters. We used this modified algorithm to develop an economic model for Ghana. We assessed the validity of this clustering methodology by comparing cluster differences in mean child HAZ, women's literacy, and child mortality.

Results: Agglomerative hierarchical clustering aggregated the twenty Cameroonian economic clusters into two rural and four urban groups based on cluster similarities in child HAZ, women's literacy, and child mortality. The differences between adjacently ranked groups across all three metrics were statistically significant ($p<0.05$) except for the difference in child mortality between the urban middle-class tenants and the urban wealthy ($p=0.12$). Using a minimum threshold ASW of 0.70, the EconomicClusters algorithm generated an economic model for Ghana consisting of two rural and three urban economic clusters. The differences between adjacently ranked economic groups based on child HAZ, women's literacy, and child mortality were statistically significant ($p<0.05$) for most but not all of the Ghanaian economic groups. However, cluster mean values of these socioeconomic variables demonstrated a consistent ordinal ranking system for the Ghanaian economic clusters across all three variables.

Conclusions: The modified EconomicClusters algorithm defined five and six economic groups respectively for Ghana and Cameroon that were associated in a consistent manner with child HAZ, women's literacy scores, and child mortality rates. This improved EconomicClusters model could facilitate health disparities research in any country with DHS data by generating simple, ordinally ranked, population-specific economic models that are feasible to assess in time-constrained settings and that correlate with diverse health and socioeconomic variables.

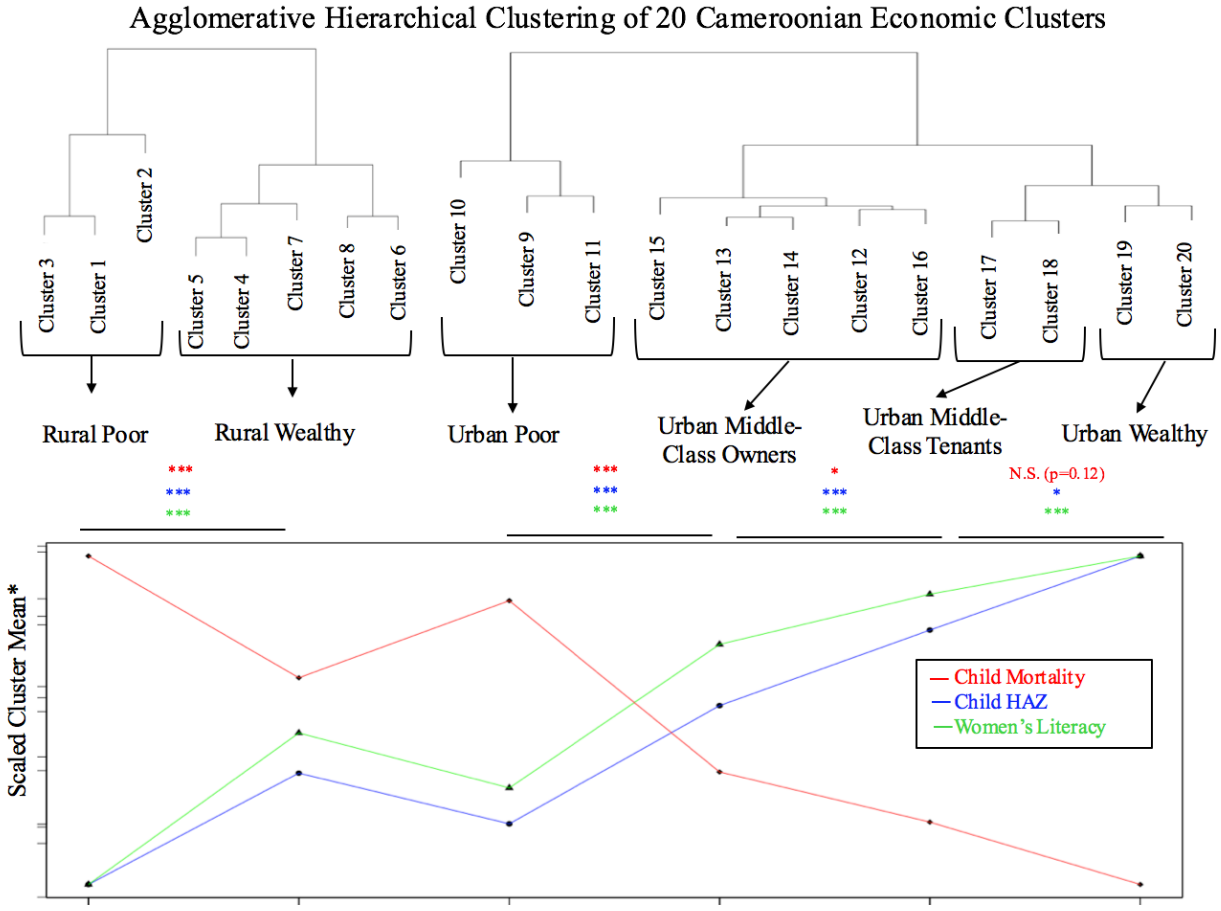

Significance levels for unpaired student's t-tests: *=p<0.05, **=p<0.01, ***=p<0.005
***Scaled cluster mean values for the following variables:**
Child Mortality defined as proportion of a woman's children who are deceased
Child HAZ = child height-for-age Z-Score
Women's Literacy Score: 0="Cannot read at all", 1="Able to read only parts of a sentence", 2="Able to read whole sentence"

Residents Learning Robotic Technology: Turning a Complicated Process into an Opportunity for Progress

Green, Courtney A.; Chu, Simon; Mahuron, Kelly; Harris, Hobart; Chern, Hueylan; O'Sullivan, Patricia

INTRODUCTION: Understanding the process of surgical skill acquisition in robotic-assisted surgeries requires a series of studies. After identifying the status of current robotic curriculum, we interviewed academic surgeons to determine what challenges they faced integrating residents with robotic technology. From interviews of 24 robotic surgeons involved in resident teaching, four major themes we identified: techniques versus tool, timing of exposure, overlapping features, and use of the dual console. Each theme generated an associated recommendation. Based on the recommendations for the two themes of technique vs. tool and the use of the dual console as a unique teaching tool, we modified our previously designed UCSF resident robotic curriculum. This study describes our curricular modifications and the subsequent evaluation of the implementations.

METHODS: The modified curriculum involved two major activities: a dry-lab for junior residents to practice robotic docking and instrument exchange and a wet-lab for senior residents to practice operating with the robot on live tissue. We modified our previous R2 curriculum, initially designed to teach and document proficiency of robotic docking and instrument exchange, to include instrument collisions, a recommendation stemming from the theme of separating the technique vs tool. After completing the dry-lab, participants completed retrospective post-course surveys. For comparison, PGY-matched urology trainees who did not participate but do work with robotic technology in the operating room also completed a survey. To address recommendations from the dual console as a unique teaching tool theme, we observed robotic surgeons as they guided surgical residents through an operative session using live porcine tissue and the da Vinci Surgical System (Intuitive Surgical, Sunnyvale CA). Observers documented the language, gestures and behaviors occurring at these stations. Using qualitative content analysis, we summarize the type and frequency of teaching behaviors and we compared our results to behaviors used in open and laparoscopic surgery. Focus groups were conducted after the session for both residents and faculty to discuss strengths and weakness of the wet lab.

RESULTS: After the dry-lab, residents reported improved knowledge and confidence in 5 domains reflecting session objectives ($p<0.05$). Residents completing the session could list and troubleshoot collisions significantly more than their non-participant matched peers ($p <0.05$). The wet lab activity revealed robotic surgeons used 11 of 16 previously identified teaching behaviors. Behaviors did not vary by surgical specialty or experience, but distribution differed from behaviors observed in open and laparoscopic instructional settings. While some categories were not applicable for robotic surgery, other behaviors increased in use. Additionally, we identified robotic-specific behaviors that involved disengaging the resident from the operative console for either onscreen direction or for gesturing with verbal instruction. In the focus groups, both faculty and residents emphasized that they highly valued the wet lab's opportunity for practice.

CONCLUSION: Robotic skill acquisition throughout surgical residency illustrates a multifaceted learning process. After identifying current curricular models and challenges with integrating the technology into training, we revised the UCSF curriculum to target some of these themes. Results suggest the curricular activities provided valuable opportunities outside of the operating room for trainees to improve their robotic confidence and skill acquisition. Additionally, educators used different teaching behaviors when engaging in robotic instruction. Faculty valued the opportunity to practice these robotic instruction techniques in the wet lab. Opportunities for faculty development warrant further investigation.

Preclinical Surgical Experience with an Intervascular Hemofilter for Organ Replacement Therapy

Authors:
J Moyer, N Wright, C Blaha, J Ly, A Santandreu, W Fissell, S Vartanian, S Roy

Purpose:
Intervascular bioartificial organs depend on high-efficiency hemofiltration for immune-privileged convective mass transfer. We sought to optimize implantation of a silicon nanopore membrane (SNM)-based hemofilter (HF) for renal and pancreatic islet replacement therapy.

Methods:
We performed a proof-of-concept study to refine HF design and implantation considerations, enabling long-term HF patency. A swine model was chosen to approximate human vascular anatomy and thrombogenesis. HF prototypes housing SNM were implanted in arteriovenous fashion to the vasculature, enabling iterative assessment of HF characteristics: implantation technique, blood flow path, vessel-graft-device interface, and ultrafiltrate (UF) drainage. Patency was assessed by physical exam, Doppler ultrasound, and fluoroscopy.

Results:
A HF was designed to eliminate high- and low-shear flow conditions using computational fluid dynamics (CFD) modeling, and subsequently constructed from polycarbonate and SNM. The prototype HF was attached via polycarbonate barbed connector to ePTFE vascular grafts anastomosed to the swine vasculature. UF was drained into a vein or externalized for collection or renal replacement. Initial patency was 50% (4/8). Changes in HF implantation including: use of a stainless steel barbed graft connector, silicone radial reinforcement of ePTFE grafts, alterations in surgical technique, and application of an anti-thrombotic UF catheter resulted in improved HF functionality, and 80% patency (8/10) up to 26 days' duration. In summary, HF and surgical refinement resulted in durable patency and function, establishing a platform for development of hemofiltration-based bioartificial organs.

Machine Learning Without Borders? An Adaptable Tool to Optimize Mortality Prediction in Diverse Clinical Settings

S. Ariane Christie MD, Alan E Hubbard PhD, Morad Hameed MD MPH, Rochelle A. Dicker MD, Rachael A Callcut MD MSPH, Fanny Nadia Dissak-Delon, Mitchell Jay Cohen MD, Catherine Juillard MD MPH

Introduction: Mortality prediction aids clinical decision-making and is necessary for quality improvement initiatives. Validated metrics rely on pre-specified variables and often require advanced diagnostics which are unfeasible in resource-constrained contexts. We hypothesize that machine learning will generate superior mortality prediction in both high-income(HIC) and low and middle-income country(LMIC) cohorts.

Methods: SuperLearner(SL), an ensemble machine-learning algorithm, was applied to data from three prospective trauma cohorts: a highest-activation cohort in the United States(US), a high-volume center cohort in South Africa(SA), and a multicenter registry in Cameroon. Cross-validation was used to assess model discrimination of discharge mortality by site using receiver operating characteristic curves. SuperLearner discrimination was compared with standard scoring methods. Clinical variables driving SL prediction at each site were evaluated.

Results: Data from 28,212 injured patients were used to generate prediction. Discharge mortality was 17%, 1.3%, and 1.7% among US, SA, and Cameroonian cohorts. SL delivered superior prediction of discharge mortality in the US (AUC 94-97%) and vastly superior prediction in Cameroon (AUC 90-94%) compared to conventional scoring algorithms. It provided similar prediction to standard scores in the SA cohort (AUC 90-95%). Context-specific variables (partial thromboplastin time in the US and hospital distance in Cameroon) were prime drivers of predicted mortality in their respective cohorts, while severe brain injury predicted mortality across sites.

Conclusions: Machine learning provides excellent discrimination of injury mortality in diverse settings. Unlike traditional scores, data-adaptive methods are well-suited to optimizing precise site-specific prediction regardless of diagnostic capabilities or dataset inclusion allowing for individualized decision-making and expanded access to quality improvement programming.

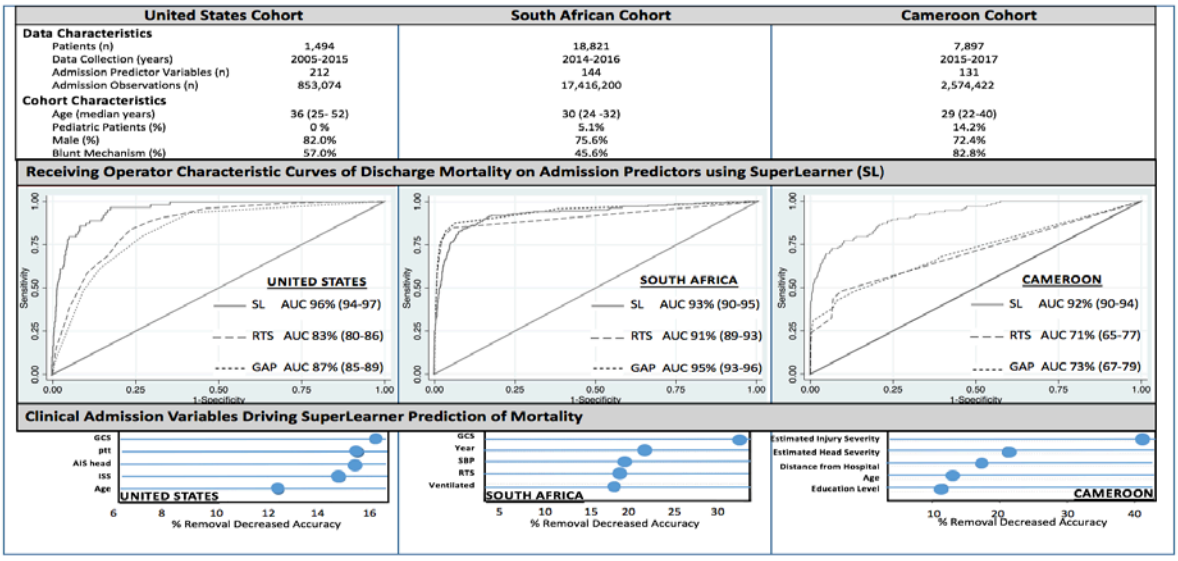

A Magnetic Jejunoileal Partial Diversion in Nonhuman Primates: A Novel Approach in Metabolic Surgery

Authors: Patel VH, Kwiat D, Leeflang E, Graham J, Havel PJ, Harrison MR.

Introduction:
We hypothesize that a jejunoileal anastomosis and partial diversion using Magnamosis, a novel magnetic compression device, is technically feasible and will improve insulin resistance and metabolic syndrome. Metabolic surgery has demonstrated improvements in various parameters including insulin resistance, triglyceride levels, and cholesterol. It may be possible to perform a less-invasive operation through partial diversion, and thereby stimulate an increase in incretins from the L-cells of the ileum to glean these benefits.

Methods:
We performed a laparotomy and jejunoileal partial diversion using Magnamosis in five Rhesus macaques with induced insulin resistance through dietary modifications. After surgery, weight was monitored and timed tests were performed at baseline and again at 3 and 6 weeks postoperatively for triglyceride levels, GLP-1, insulin, glucose, and bile acids. The primates were followed for 8 weeks prior to euthanasia. Results are represented as mean (SD) and all p-values were calculated using a two-sample Students' t-test.

Results:
All five monkeys successfully underwent surgery without technical or postoperative complications. Mean weight at 8 weeks decreased from baseline 17.9 (2.6) kg to 15.1 (3.4) kg (p=0.067), for a mean weight loss of 9.6%. At 6 weeks, there was a statistically significant decrease in mean triglyceride levels from 354.0 (12.2) mg/dL to 83.6 (4.0) mg/dL ($p=9.8x10^{-15}$), mean fasting glucose from a baseline of 68.2 (13.8) mg/dL to 60.3 (9.4) mg/dL (p=0.0066), and fasting insulin from 96.4 (19.1) µU/mL to 35.2 (7.0) µU/mL ($p=1.7x10^{-6}$). At 6 weeks, bile acid levels increased from 4.4 (1.2) µmol/L to 6.0 (0.4) µmol/L ($p=5.93x10^{-7}$). Additionally, at 3 weeks, GLP-1 Active levels increased from the mean baseline value of 2.1 (0.6) ρg/mL to 7.0 (2.9) ρg/mL ($p=4.5x10^{-7}$). Due to unanticipated effects of anesthesia during the timed mixed meal tolerance and oral glucose tolerance tests, we were unable to effectively demonstrate an improvement in insulin resistance

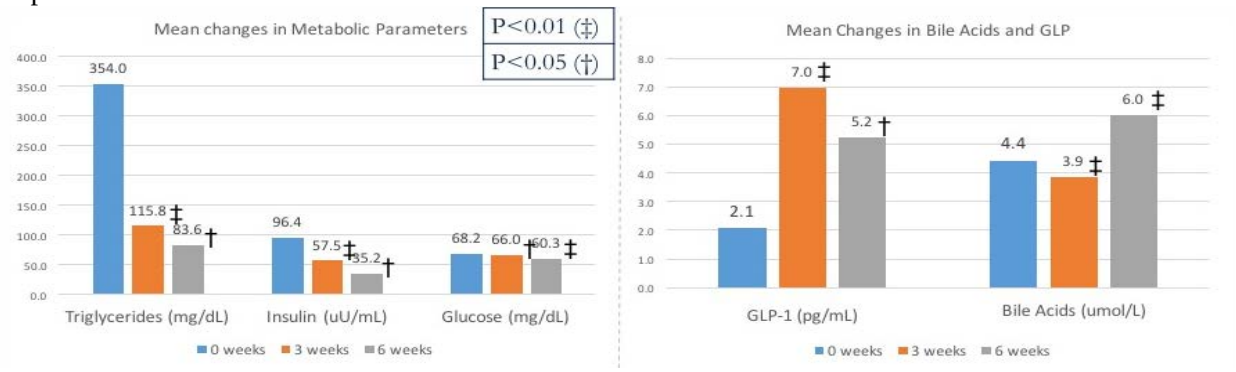

Conclusions:
The creation of a magnetic jejunoileal partial diversion in the rhesus monkey is technically feasible and reproducible. The translational similarities between the rhesus macaque metabolome and humans demonstrated expected improvements in specific metabolic parameters and GLP-1. In order to develop a more effective translational metabolic model and demonstrate a clear improvement in insulin resistance, we are performing a new study to evaluate the effects of this operation in ten Rhesus macaque.

The Impact of Incisional Negative Pressure Wound Therapy on Wound Healing Complications in the Groin

Clara Gomez-Sanchez, Merisa Piper, Romina Deldar, Jacquelyn Withers, Rachel Lentz, Hani Sbitany, Scott Hansen

Introduction:

Vascular procedures with incisions in the groin have a high rate of wound healing complications, and high-risk patients have been previously shown to benefit from collaboration with plastic surgeons for closure with a rotational muscle flap. In recent years, incisional negative pressure wound therapy devices (iNPWT) have become commercially available and are proposed to further decrease rates of wound complications. We hypothesize that the use of iNPWT on groin incisions for open vascular procedures closed by plastic surgery will decrease the overall rate of wound healing complications.

Methods:

This is a pre-post cohort study comparing rates of wound healing complications among patients undergoing open vascular procedures in the groin with incisions closed using a rotational muscle flap by plastic surgery. The experimental group was prospectively recruited to have the Prevena™ (KCI, an Acelity company, San Antonio, Tex.) negative pressure wound device placed at the end of surgery, with retrospective review of historical controls during the year prior to the start of the study.

Progress:

Twenty-five patients with 31 operative groins have been recruited into the experimental group thus far (study powered for 58). The groups are well matched in terms of comorbid conditions and operative details. On analysis of preliminary data, there has been a significant reduction in overall wound complications in the iNPWT group (major and minor, 26.67% vs 58.06% p=0.013). Rates of cellulitis and skin dehiscence have also been reduced but have not reached statistical significance (10.0% vs 25.58% p=0.19 and 16.67% vs 35.48% p=0.10, respectively). There has been a trend towards fewer readmissions and reoperations in the iNPWT cohort that has not reached significance (6.67% vs 19.35% p=0.14 and 3.33% vs 16.13% p=0.09, respectively).

Conclusions:

The impact of iNPWT is promising in the reduction of wound healing complications following open vascular procedures in the groin in high-risk patients. The study is not yet adequately powered and recruitment of more patients is required. In addition, some of the experimental group has not yet completed the entire follow-up period, and may still present with wound healing complications.